CAPITAL UNIVERSITY OF SCIENCE AND TECHNOLOGY, ISLAMABAD

Squeezing Flow of Tangent Hyperbolic Fluid over a Sensor Plate

by

Hamid Rehman

A thesis submitted in partial fulfillment for the degree of Master of Philosophy

in the

Faculty of Computing
Department of Mathematics

2019

Dedication of this thesis to my lovely Mom. Miss you Mom

CERTIFICATE OF APPROVAL

Squeezing Flow of Tangent Hyperbolic Fluid over a Sensor Plate

by

Hamid Rehman

(MMT161001)

THESIS EXAMINING COMMITTEE

S. No.	Examiner	Name	Organization
(a)	External Examiner	Dr. Tanvir Akber Kiani	CIIT Islamabad
(b)	Internal Examiner	Dr. Shafqat Hussain	CUST Islamabad
(c)	Supervisor	Dr. Muhammad Sagheer	CUST Islamabad

Dr. Muhammad Sagheer
Thesis Supervisor
October, 2019

Dr. Muhammad Sagheer
Head
Dept. of Mathematics
October, 2019

Dr. Muhammad Abdul Qadir
Dean
Faculty of Computing
October, 2019

Author's Declaration

I, **Hamid Rehman** hereby state that my M. Phil thesis titled "**Squeezing Flow of Tangent Hyperbolic Fluid over a Sensor Plate**" is my own work and has not been submitted previously by me for taking any degree from Capital University of Science and Technology, Islamabad or anywhere else in the country/abroad.

At any time if my statement is found to be incorrect even after my graduation, the University has the right to withdraw my M. Phil Degree.

(Hamid Rehman)

Registration No: MMT161001

Plagiarism Undertaking

I solemnly declare that research work presented in this thesis titled "**Squeezing Flow of Tangent Hyperbolic Fluid over a Sensor Plate**" is solely my research work with no significant contribution from any other person. Small contribution/help wherever taken has been dully acknowledged and that the complete thesis has been written by me.

I understand the zero tolerance policy of the HEC and Capital University of Science and Technology towards plagiarism. Therefore, I as an author of the above titled thesis declare that no portion of my thesis has been plagiarized and any material used as reference is properly referred/cited.

I undertake that if I am found guilty of any formal plagiarism in the above titled thesis even after the award of M. Phil degree, the University reserves the right to withdraw/revoke my M. Phil degree and that the HEC and the University have the right to publish my name on the HEC/University website on which names of students are placed who submitted plagiarized work.

(Hamid Rehman)

Registration No: MMT161001

Acknowledgements

All praise is for the most merciful Almighty Allah. Most powerfully and creator to every thing in the universe. Thankful to my Almighty Allah to give me great opportunity to completed my thesis. In the whole work in my thesis to involved the helped and idea of the great merciful Almighty Allah. Also, I cannot forget the idea of the most talented unique personalty say to namely prophet **Muhammad (Sallallahu Alaihay Wa'alihi wasalam)** for whom Allah to created the universe.

I would like to expressed my heart-felt word for the my respected supervisor **Dr. Muhammad Sagheer**, Head of Mathematics Department, Capital University of Science and Technology, Islamabad to suggested my research problem. His guidance and helped to me every moment to solve problem and writing my thesis. Also, I would like thank to my respected teachers **Dr. Shafqat Hussain and Dr. Muhammad Afzal**.

Finally, dedication of my thesis award goes to my lovely parents and all family members who appreciate, supporting and motivate me to every moment of my education life. I would like thank to beloved friends **Mr. Ateeq-ur-Rehman and Mr. Raz Muhammad** who guided me through the successful writing this thesis. God blessings, prosperity on all those who encouragement me through completion of this thesis.

(Hamid Rehman)

Registration No: MMT161001

Abstract

The aim of this thesis is to analyze the thermal radiation and heat effects on two-dimensional unsteady squeezed flow of a tangent hyperbolic fluid flow towards a sensor surface. The governing nonlinear boundary value problem involving the partial differential equations is reduced to a system of nonlinear ordinary differential equations by using appropriate similarity transformations. The nonlinear boundary values problem is solved numerically by using well known shooting technique scripted in the computational software Matlab. The impact of different physical parameters on skin friction, Nusselt number is exhibited and analysed graphically. The variations in the power-law index, the permeable velocity parameter and Weissenberg number are observed to influence the skin friction coefficient and Nusselt number, very prominently.

Contents

List of Figures

List of Tables

Abbreviations

BVPs	Boundary value problems
IVPs	Initial value problems
MHD	Magnetohydrodynamics
ODEs	Ordinary differential equations
PDEs	Partial differential equations
RK	Runge-Kutta

Symbols

s	Arbitrary Constant
ρ	Density
σ	Electric Charge Density
μ	Fluid Viscosity
T_∞	Free Stream Temperature
u, v	Velocity Components
ν	kinematic Viscosity
U	Free Stream Velocity
ψ	Free Stream Function
$q_0(t)$	Heat Flux
M	Magnetic Parameter
B_0	Magnetic Filed
Nu_x	Nusselt Number
n	Power Law Index
P	Pressure
f_0	Permeable Velocity
Pr	Prandtl Number
a	Strength of Squeezed Flow Parameter
ϵ	Small Quantity
C_f	Skin Friction
C_p	Specific Heat
b	Squeezed Flow Index
τ	Stress Tensor

α	Thermal Diffusivity
Γ	Time Dependent Constant
T	Temperature
t	Time
Rd	Thermal Radiation
K	Thermal Conductivity
$\alpha(T)$	Variable Thermal Conductivity
W_e	Weissenberg Number

Chapter 1

Introduction

Squeezed flow is a special type of flow which occurs between two plates in such a way that at least one of the two is moving towards the other. It plays an important role in fluid mechanics, engineering, biology and its many applications can be found even at industrial level such as production of various types of foods, injection molding and many uses in other technologies. Moore [1] analyzed the squeezed phenomena for the viscous non-Newtonian fluid flow between two approaching plane surfaces. Wang [2] discussed the unsteady squeezing viscous fluid flow between two circular plates. Wang [3] investigated the dynamics of a fluid inside a tube squeezing at arbitrary rates with small squeeze number. Usha and Sridharan [4] tested the arbitrary squeeze of viscous fluid flow passing through a space between two elliptic plates. Further studies related to the the heat transfer of a squeezing flow by many researchers can be seen in [5–8].

The scrutiny of heat and mass transfer in many industrial and sensible applications in peculiar areas like nuclear reactors, chemical reaction, solar energy in space technology, polymer exclusion, energy production, production of pharmacology aim a drag and used others technologies. Mahmood et al. [9] analyzed the heat and mass transposition in squeezing channel of viscous fluid flow towards a permeable surface. Lin et al. [10] presented the characteristics of electromagnetic squeezed fluid flow surrounding the annular curved sheet. Hamza [11] discussed

the magnetic filed and centrifugal force effects on a squeezed fluid flow film inside two parallel rotating disks. In case of low viscosity lubricants which reduce the energy losses. Khaled and Vafai [12] marked the magnetohydrodynamics effect on the squeezed fluid flow subjected to the heterogeneity transformation inside the porous medium. Siddiqui et al. [13] investigated the viscous MHD effect on a fluid flowing under the influence of an electromagnetic filed. Hayat et al. [14] discussed magnetohydrodynamics unsteady non-Newtonian flow of a squeezed fluid over a porous medium in a starching surface. Ahmed et al. [15] studied the free convection flow of unsteady MHD fluid along with the heat source and thermal diffusion involving porous surface.

The applications of thermal radiation heat transfer can be found in engineering, manufacturing processes, chemical reactions, semiconductors and many others technologies. Sohn and Chen [16] concluded that the microconvection thermal effect in two phase mixtures is more effective than that for the single phase fluid at a shear flow. Makinde [17] studied the free convection flow with the presence of thermal radiation and mass transfer passing through a permeable vertical surface. Hayat et al. [18] discussed the heat transfer in unsteady squeezing Jeffery fluid flow. Hussain et al. [19] studied the thermal characteristics in bioconvection squeezing flow between two parallel plates. Further work on the effects of thermal radiation heat and mass transfer in fluid flow can be seen in [20–22].

Some important applications of non-Newtonian fluids can be seen in different areas like thermoplastic processing, oil, food production, plasma and bioscience technology. Datt and Elfring [23] pointed out that the motion of particles is different in Newtonian and non-Newtonian fluids. The rheological effects of non-Newtonian fluids are expected to be more complex than those for the Newtonian fluids. Kumar et al. [24] investigated the essential branch of non-Newtonian fluid known as the tangent hyperbolic fluids. Akbar et al. [25] analysed the analytical results of non-Newtonian tangent hyperbolic fluid flow with magnetic effect inside a stretching plate. Hayat et al. [26] discussed the thermal radiation effects with free

convective flow of heat and mass transfer in chemical burner of tangent hyperbolic fluid towards a stagnation point. Malik et al. [27] studied the non-Newtonian tangent hyperbolic fluid flow with magnetic effects inside a stretching tube.

The phenomenon of thermal conductivity of fluids can be improved by the addition of nanometer suspended particles in them. The resulting fluids are known as nano-fluids and are used for the enhancement of the heat transfer. A rise in the temperature of nanofluids can take place over a temperature range of 22^0 to 52^0. Akbar and Khan [28] studied the thermal energy effect in nanofluid flow inside a stretching permeable sheet. Saidulu et al. [29] investigated the zero normal flux of nonoparticles on MHD boundary layer flow with the effects of inclined magnetic number and viscous recreation of non-Newtonian nonofluid inside a stretching plate. Ibrahim [30] investigated the thermal effect on second-grade slip condition MHD flow of tangent hyperbolic fluid with zero normal flux of nanoparticles past through the stretching surface. Khan et al. [31] investigated the magnetohydrodynamics tangent hyperbolic nanofluid over a boundary layer flow past a stretching sheet. The research work involving the sensor surface can be found in [32].

Sensor technology is widely used in our daily life. The sensor surface applications can be found in the biological, chemical reaction processes, agriculture, weather analysis, electronic, and much more technologies, for example, wireless, remote sensor, a microphone sensor. Salahuddin et al. [33] analyzed the MHD squeezed flow through a horizontal sensor surface with the presence of Carreau-Yasuda fluid. Rout and Mishra [34] analyzed the thermal energy transport on MHD nanofluid flow over a sensor surface towards a stretching sheet. Hayat et al. [35] investigated the heat transfer in a second-grade fluid flow of squeezing channel towards a sensor surface along with the thermal conductivity. More literature regarding the sensor surface can be consulted in [36–40] applied to used the sensor surface model for the heat and mass transformation mechanisms.

1.1 Thesis Contributions

In this thesis, first the work of Kumar et al. [24] has been reviewed in detail. Discussed the present squeezing model is modified by including the effect of thermal radiation of a squeezing flow of a tangent hyperbolic fluid towards a micro cantilever sensor plat. The non-dimensional partial differential equations are reduced into the dimensionless system of ODEs by using the similarity transformation. The numerical results is access by using well known shooting technique which is working on the computational software Matlab.

1.2 Thesis Outlines

In addition to be present, this thesis is further distributed over four chapters.

Chapter 2 presents the basic laws, definitions and its properties. Moreover, the solution methodology for the basic governing equations has also been discussed.

In **Chapter 3** the work of Kumar et al. [24] has been reviewed the numerical solution on unsteady squeezing flow with tangent hyperbolic fluid towards a sensor surface.

Chapter 4 describes the extended work of Kumar et al. [24] by including the thermal radiative particles effect in the governing model.

Chapter 5 compiles the major findings of the thesis.

All relevant references are shown in **Bibliography**.

Chapter 2

Basic Definitions and Governing Laws

In this chapter, some basic laws and terminologies are presented which will be used with subsequent chapters. The relevant definitions regarding fluid flow and its properties have been taken from [41], [42], [43]. The material included in this chapter will be helpful for understanding the rest of the thesis.

2.1 Fluid

"There is a physical law that a substance exists in three primary phases solid, liquid, and gas. A substance in the liquid or gas phase is referred to as a fluid. Distinction between a solid and a fluid is made on the basis of the substance's ability to resist an applied shear stress that tends to change its shape. A solid can resist an applied shear stress by deforming, whereas a fluid deforms continuously under the influence of shear stress, no matter how small. In solids stress, is proportional to strain, but in fluids stress is proportional to strain rate."

2.2 Fluid Mechanics

"Fluid mechanics is that branch of science which deals with the behaviour of the fluids (liquids or gases) at rest as well as in motion. Thus this branch of science deals with the study of kinematic and dynamic aspects of fluids. The study of fluids at rest is called statics. The study of fluids in motion, where pressure forces are not considered, is called fluid kinematics and if the pressure forces are also considered for the fluids in motion, that branch of science is called fluid dynamics."

2.3 Fluid Dynamics

"Fluid dynamics is the branch of applied science that is concerned with the movement of liquids and gases. Fluid dynamics is one of two branches of fluid mechanics, which is the study of fluids and how forces affect them. (The other branch is fluid statics, which deals with fluids at rest)."

2.3.1 Mass Density

"The density of a fluid, designated by the Greek symbol ρ (rho), is defined as its mass per unit volume. Density is typically used to characterize the mass of a fluid system. In the BG system, ρ has units of slugs/ft^3 and in SI the units are kg/m^3. The value of density can vary widely between different fluids, but for liquids, variations in pressure and temperature generally have only a small effect on the value of ρ. Mathematically type as

$$\rho = \frac{\text{Mass of fluid}}{\text{Volume of fluid}}, \tag{2.1}$$

The value of density of water is 1 gm/cm^3."

2.3.2 Stress Field

"Surface forces on a fluid particle lead to stresses. The concept of stress is useful for describing how forces acting on the boundaries of a medium (fluid or solid) are transmitted throughout the medium."

2.3.3 Surface Tension

"These various types of surface phenomena are due to the unbalanced cohesive forces acting on the liquid molecules at the fluid surface. Molecules in the interior of the fluid mass are surrounded by molecules that are attracted to each other equally. However, molecules along the surface are subjected to a net force towards the interior. The apparent physical consequence of this unbalanced force along the surface is to create the hypothetical skin or membrane. A tensile force may be considered to be acting in the plane of the surface along any line in the surface. The intensity of the molecular attraction per unit length along any line in the surface is called the surface tension and is designated by the Greek symbol σ."

2.3.4 Dynamic Viscosity

"It is the resistance of the substance to flow. It depends upon the size and shape of molecules. It is related with the concept of shear force. Mathematically, it is denoted by μ. Examples are honey, oil.

$$\mu = \frac{\text{shear stress}}{\text{shear strain}}. \tag{2.2}$$

It is denoted by μ. Viscosity is the rate of shear strain or shear stress deformation."

2.3.5 Kinematic Viscosity (ν)

"Kinematic viscosity is the ratio of the dynamic viscosity μ to the mass density ρ. The kinematic viscosity can be obtained by dividing the absolute viscosity of a fluid with the fluid mass density. It is denoted by the Greek letter ν. Mathematically, we can write"

$$\nu = \frac{\mu}{\rho}. \tag{2.3}$$

2.3.6 Viscosity vs Friction

"Friction and viscosity refer to the forces that oppose the motion. The main difference between friction and viscosity is that friction is used to refer to forces that resist relative motion, in general, whereas viscosity refers specifically to resistive forces that occur between layers of a fluid when fluids attempt to flow. Therefore, the term friction can also be referred to as the resistive force between solid surfaces, or the resistive forces between solid and fluid surfaces."

2.4 Properties of Fluids

2.4.1 Ideal Fluids

"Consider a hypothetical fluid having a zero viscosity μ=0. Such a fluid is called an ideal fluid and the resulting motion is called as ideal or inviscid flow. In an ideal flow, there is no existence of shear force because of vanishing viscosity. Mathematically, it is denoted by"

$$\tau = \mu \frac{du}{dy} = 0 \quad since \;\; \mu = 0. \tag{2.4}$$

2.4.2 Real Fluid

"A fluid, which possesses viscosity, is known as a real fluid. All the fluids, in actual practice, are real fluids."

2.4.3 Newtonian Fluid

"A fluid in which the viscous stresses that arises from its flow are linearly proportional to the strain, i.e., the rate of change of its deformation, as shear stress and the rate of deformation are directly proportional to each other is called as Newtonian fluids. In other words, the fluid which obeys the Newton's law of viscosity are called Newtonian fluids. Mathematically, denoted as

$$\tau_{yx} = \mu \frac{du}{dy}, \tag{2.5}$$

where τ is the shear stress, u is the velocity, μ is the viscosity of fluid. Example of Newtonian fluid are glycerol and silicone/thin motor oil."

2.4.4 Non-Newtonian Fluid

"When shear stress is not directly proportional to the velocity gradient are defined as non-Newtonian fluid. In other words, the fluid which does not obey the Newton's law of viscosity is said to be non-Newtonian fluids. i.e. Toothpaste, ketchup, Shampoo and Blood etc. Mathematically, it can be expressed."

$$\tau_{yx} = \mu \left(\frac{du}{dy} \right)^{n} \quad n \neq 1 \tag{2.6}$$

2.4.5 Tangent Hyperbolic Fluid [44]

"Tangent hyperbolic fluid model is a particular type of non-Newtonian fluid which is used extensively for different laboratory experiments."

2.4.6 Compressible vs Incompressible

"A fluid is a substance that can flow easily. A fluid has no definite shape and it takes the shape of the container which it is occupied. There are very weak attraction forces between molecules of the fluid. Gas and liquid phases are considered as fluids mainly due to their ability to flow. Gases are called compressible fluid whereas liquids are called incompressible fluid. The main difference between compressible and incompressible fluid is that a force applied to a compressible fluid changes the density of the a fluid whereas a force applied to an incompressible fluid does not change the density to a considerable degree."

2.5 Flow

"The movement of liquids and gases is generally referred to as flow, a concept that describes how fluids behave and how they interact with their surrounding environment i.e., water moving through a channel or pipe, or over a surface. Flow can be either steady or unsteady."

2.5.1 Steady vs Unsteady

"If all properties of a flow are independent of time, then the flow is steady, otherwise, it is unsteady. That is, steady flows do not change over time. An example of steady flow would be water flowing through a pipe at a constant rate. But if all properties of a flow are dependent of time , then the flow is unsteady. An example of unsteady flow would be water pouring from an old-fashioned hand pump are examples of unsteady flow."

2.5.2 Laminar vs Turbulent

"The flow of fluid, when each particle of the fluid follows a smooth path. The laminar flow is that the velocity of the fluid is constant at any point. But The

turbulent flow is define as the fluid particles is moving irregular flow characterized by the tiny whirlpool region. The velocity of turbulent flow is not constant at every point."

2.5.3 Boundary Layer Flow

"The concept of boundary layer was first introduced by a German scientist, Ludwig Prandtl, in the year 1904. Although, the complete descriptions of motion of a viscous fluid were known through Navier-Stokes equations, the mathematical difficulties in solving these equations prohibited the theoretical analysis of viscous flow. Prandtl suggested that the viscous flows can be analysed by dividing the flow into two regions; one close to the solid boundaries and other covering the rest of the flow. Boundary layer is the regions close to the solid boundary where the effects of viscosity are experienced by the flow. In the regions outside the boundary layer, the effect of viscosity is negligible and the fluid is treated as inviscid. So, the boundary layer is a buffer region between the wall below and the inviscid free-stream above."

2.5.4 No-Slip Boundary Layer Flow

"In fluid dynamic the no-slip condition for viscous fluids assumes that at a solid surface boundary, the velocity at this region will be zero if the viscous fluids velocity is equal to the solid boundary."

2.5.5 Thermal Boundary Layer Flow

"In fluid dynamic thermal boundary layer flow is defined as the heat transfer of the boundary layer thickness of the fluid and wall of the solid surface at this region is called thermal boundary layer flow."

2.6 Type of Heat Transfer [45]

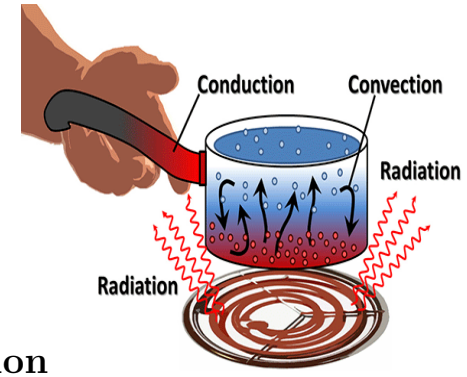

2.6.1 Conduction

"Conduction transfers heat via direct molecular collision. An area of greater kinetic energy will transfer thermal energy to an area with lower kinetic energy. Higher-speed particles will collide with slower speed particles. The slower-speed particles will increase in kinetic energy as a result. Conduction is the most common form of heat transfer and occurs via physical contact. Examples would be to place your hand against a window or place metal into an open flame."

2.6.2 Convection

"When a fluid, such as air or a liquid, is heated and then travels away from the source, it carries the thermal energy along. This type of heat transfer is called convection. The fluid above a hot surface expands, becomes less dense, and rises."

2.6.3 Radiation

"Thermal radiation generates from the emission of electromagnetic waves. These waves carry the energy away from the emitting object. Radiation occurs through a vacuum or any transparent medium (either solid or fluid). Thermal radiation is the direct result of random movements of atoms and molecules in matter. Movement of the charged protons and electrons results in the emission of electromagnetic radiation."

2.6.4 Thermal Conductivity

"Thermal conductivity is a material property that describes ability to conduct heat. Thermal conductivity can be defined as the quantity of heat transmitted through a unit thickness of a material in a direction normal to a surface of unit area due to a unit temperature gradient under steady state conditions. Mathematically, written as

$$k = \frac{QL}{A\Delta T} \tag{2.7}$$

where, k is thermal conductivity in $[W/mK]$ in the SI system, Q is amount of heat transfer through the material in J/S or W, A is the area of the body in m^2, $\Delta\ T$ is difference in temperature in K."

2.6.5 Thermal Diffusivity

"It can be defined thermal diffusivity is a material-specific property for characterizing unsteady heat conduction. This value describes how quickly a material reacts to a change in temperature. Mathematically,

$$\alpha = \frac{k}{\rho C_p}, \tag{2.8}$$

where k is the thermal conductivity of a material, ρ is the density and C_p is the heat capacity. The unit of the thermal diffusivity are m^2s^{-1} in the SI system and dimensional form is $[L^2T^{-1}]$ respectively."

2.7 Basic Governing Equations

2.8 Conservation of Mass

"The conservation of mass relation for closed system. Obvious that the mass of system remains constant during a process. For a control volume, mass balance is

expressed in the rate form as

$$\text{Conservation of mass} \quad m_{in} - m_{out} = \frac{dm_{cv}}{dt} \tag{2.9}$$

where m_{in} and m_{out} are the total rates of mass flow into and out of the control volume, respectively, and dm_{cv}/dt is the rate of change of mass within the control volume boundaries. In fluid mechanics, the conservation of mass relation written for a differential control volume is usually called the continuity."

2.8.1 Conservation of Momentum

"The product of the mass and the velocity of a body is called the linear momentum or just the momentum of the body, and the momentum of a rigid body of mass m moving with a velocity V is mV. Newton's second law states that the acceleration of a body is proportional to the net force acting on it and is inversely proportional to its mass, and the rate of change of the momentum of a body is equal to the net force acting on the body.therefore the momentum of a system remains constant when the net force acting on it is zero. and thus the momentum of such systems is conserved. This is known as the conservation of momentum principle. In fluid mechanics, Newton's second law is usually referred to as the linear momentum equation."

2.8.2 Conservation of Energy

"Energy can be transferred to or from a closed system by heat or work, and the conservation of energy principle requires that the net energy transfer to or from a system during a process be equal to the change in the energy content of the system. Control volumes involve energy transfer via mass flow also, and the conservation of energy principle, also called the energy balance, is expressed as

$$\text{Conservation of energy} \quad E_{in} - E_{out} = \frac{dE_{cv}}{dt}, \tag{2.10}$$

where E_{in} and E_{out} are the total rates of energy transfer into and out of the control volume, respectively, and dE_{cv}/dt is the rate of change of energy within the control volume boundaries. In fluid mechanics, we usually limit our consideration to mechanical forms of energy only."

2.8.3 Dimension and Units

"We refer to physical quantities such as length, time, mass, and temperature as dimensions. In terms of a particular system of dimensions, all measurable quantities are subdivided into two groupsprimary quantities and secondary quantities. We refer to a small group of dimensions from which all others can be formed as primary quantities, for which we set up arbitrary scales of measure. Secondary quantities are those quantities whose dimensions are expressible in terms of the dimensions of the primary quantities. For example, length is a dimension, but centimetre is a unit."

2.8.4 Prandtl Number [46]

"Prandtl number Pr, is a characteristic of the fluid only it is dimensionless parameter. It is the ratio of kinematic viscosity to its thermal diffusivity in a fluid. Physically Prandtl number proved Mathematically, we can written as

$$Pr = \frac{\nu}{\alpha}, \tag{2.11}$$

where ν is the Kinematic viscosity and α is the thermal diffusivity respectively."

2.8.5 Skin Friction

"The systematic calculation yields the flow variables in the boundary layer including the velocity gradient at the wall surface. The shear stress at the wall, hence the

skin-friction drag on the surface, is obtained directly from those velocity gradients. It is denoted by C_f and defined as.

$$C_f = \frac{2\tau_w}{\rho U_w^2}, \tag{2.12}$$

where τ_w is the shear stress at the wall, ρ the density, and U_w the free stream velocity gradient."

2.8.6 Nusselt Number

"Nusselt number may be viewed as the ratio of the conduction resistance of a material to the convection resistance of the same material."

$$Nu_x = \frac{\text{convection heat transfer strength}}{\text{conduction heat transfer strength}} = \frac{hx}{k}. \tag{2.13}$$

Chapter 3

Unsteady Squeezing Flow of a Non-Newtonian Tangent Hyperbolic Fluid over a permeable Surface

3.1 Introduction

In this chapter, two-dimensional incompressible squeezing flow of an unsteady tangent hyperbolic fluid towards a sensor plate with uniform magnetic field has been investigated. Further, the heat transfer analysis is carried out under the influence of variable thermal conductivity. The non-dimensional governing equations are reduced into the dimensionless form of ODEs by using the following similarity transformations. The boundary values problem is solved numerically by using well known shooting technique which is working on the computational software Matlab. Graphical results are produced for some important governing parameters. The behaviour of fluid is also discussed through numerical results of skin-friction and Nusselt number.

3.2 Mathematical Problem

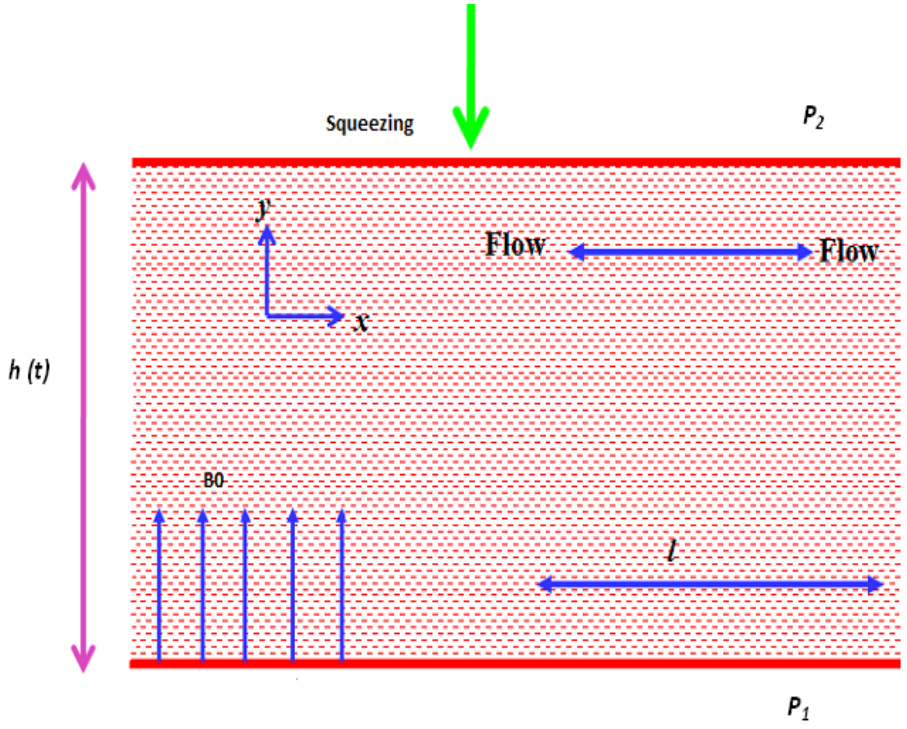

FIGURE 3.1: Model of squeezed flow over sensor plate

Consider two-dimensional incompressible boundary layer flow of an unsteady tangent hyperbolic fluid between two parallel plates P_1 and P_2. Figure 3.1 has shown that a channel with hight $h(t)$ is squeezed. It is further assumed that $h(t)$ is much larger than the boundary layer thickness. A micro-cantilever sensor of length l is assumed to be enclosed within the channel. The plate P_1 is kept fixed whereas P_2 is assumed to be pushed towards the lower plate P_1. The governing equations are modeled as:

$$\frac{\partial u}{\partial x}+\frac{\partial v}{\partial y}=0, \tag{3.1}$$

$$\frac{\partial u}{\partial t}+u\frac{\partial u}{\partial x}+v\frac{\partial u}{\partial y}=-\frac{1}{\rho}\left(\frac{\partial p}{\partial x}\right)+\nu(1-n)\frac{\partial^2 u}{\partial y^2}+\sqrt{2}\nu n\Gamma\left(\frac{\partial u}{\partial y}\right)\frac{\partial^2 u}{\partial y^2}-\frac{\sigma B_0^2}{\rho}u, \tag{3.2}$$

$$\frac{\partial U}{\partial t}+U\frac{\partial U}{\partial x}=-\frac{1}{\rho}\left(\frac{\partial p}{\partial x}\right)-\frac{\sigma B_0^2}{\rho}U, \tag{3.3}$$

$$\frac{\partial T}{\partial t}+u\frac{\partial T}{\partial x}+v\frac{\partial T}{\partial y}=\frac{\partial}{\partial y}\left(\alpha(T)\frac{\partial T}{\partial y}\right), \tag{3.4}$$

From (3.3), substituting the pressure gradient in (3.2), we get the following equation:

$$\begin{aligned}\frac{\partial u}{\partial t}+u\frac{\partial u}{\partial x}+v\frac{\partial u}{\partial y}=\frac{\partial U}{\partial t}+U\frac{\partial U}{\partial x}\\ +\nu(1-n)\frac{\partial^2 u}{\partial y^2}+\sqrt{2}\nu n\Gamma\left(\frac{\partial u}{\partial y}\right)\frac{\partial^2 u}{\partial y^2}+\frac{\sigma B_0^2}{\rho}(U-u).\end{aligned} \tag{3.5}$$

The boundary conditions of the above model have been taken as:

$$\left.\begin{aligned}&y=0: u(x,y,t)=0,\ v(x,y,t)=\nu_0(t),\ -k\frac{\partial T(x,y,t)}{\partial y}=kq(x),\\ &y\to\infty: u(x,y,t)\to U(x,t),\ T(x,y,t)\to T_\infty.\end{aligned}\right\} \tag{3.6}$$

Here u is the horizontal velocity component and v is the vertical one. Moreover, p represents the fluid pressure, $U(x,t)$ the free stream velocity point, Γ the time dependent materiel constant. $\alpha(\theta)$ the variable thermal conductivity, ν the kinematic viscosity, n the power law index, ϵ a small quantity, σ the electric charge density, ρ density of fluid and $\nu_0(t)$ velocity of the sensor surface.

3.3 Transformation

The governing equations are transformed into the dimensionless system by using the following applicable transformations: [24]

$$\left.\begin{aligned}&U=ax,\ \psi=\sqrt{a\nu}xf(\eta),\ a=\frac{1}{s+bt},\ \alpha(\theta)=\alpha_\infty(1+\epsilon\theta)\ u=axf'(\eta),\\ &v=-\sqrt{a\nu}f(\eta), T=T_\infty+\theta(\eta)q_0x\sqrt{\frac{\nu}{a}},\ \eta=y\sqrt{\frac{a}{\nu}}=y\sqrt{\frac{1}{\nu(s+bt)}}.\end{aligned}\right\} \tag{3.7}$$

In the above transformations, U the free stream velocity, a the strength of squeezing flow, b the squeezing flow index, s an arbitrary constant, $q_0(x)$ the heat flux, T presents temperature behaviour, T_∞ the free stream temperature and ψ the stream function. We, now, convert the dimensional system of the governing model (3.4) and (3.5) with boundary values (3.6) into the dimensionless form by applying the above applicable transformations.

For the conversion of (3.5) into the dimensionless form, the following procedure has been followed:

- $$\begin{aligned}\frac{\partial \eta}{\partial t} &= \frac{\partial}{\partial t}\Big(\frac{y}{\sqrt{\nu}}\sqrt{\frac{1}{s+bt}}\Big)\\ &= \frac{\partial}{\partial t}\frac{y}{\sqrt{\nu}}\big(s+bt\big)^{-\frac{1}{2}}\\ &= -\frac{y}{\sqrt{\nu}}\Big(\frac{b}{2\sqrt{s+bt}}.\frac{1}{s+bt}\Big)\\ &= y\sqrt{\frac{a}{\nu}}\Big(\frac{ab}{2}\Big)\\ &= -\frac{\eta ab}{2}. \end{aligned} \tag{3.8}$$
- $$\begin{aligned}\frac{\partial u}{\partial t} &= \frac{\partial}{\partial t}\big(axf'(\eta)\big)\\ &= ax\Big(\frac{\partial f'(\eta)}{\partial \eta}\frac{\partial \eta}{\partial t}\Big) - f'(\eta)\frac{xb}{(s+bt)^2}\\ &= \Big(-a^2x\big(f''(\eta)\frac{\eta b}{2}\big) - f'(\eta)(a^2xb)\Big)\\ &= -a^2x\Big(\frac{\eta b}{2}f''(\eta) + bf'(\eta)\Big). \end{aligned} \tag{3.9}$$
- $$u\frac{\partial u}{\partial x} = a^2x\big(f'(\eta)\big)^2. \tag{3.10}$$
- $$\begin{aligned}\frac{\partial u}{\partial y} &= ax\sqrt{\frac{a}{\nu}}f''(\eta)\\ v\frac{\partial u}{\partial y} &= -a^2x\big(f(\eta)f''(\eta)\big). \end{aligned} \tag{3.11}$$
- $$\begin{aligned}\frac{\partial U}{\partial t} &= \frac{\partial}{\partial t}\Big(\frac{x}{s+bt}\Big)\\ &= \frac{-xb}{(s+bt)^2}\\ &= -a^2xb. \end{aligned} \tag{3.12}$$
- $$\frac{\partial U}{\partial x} = a. \tag{3.13}$$
- $$U\frac{\partial U}{\partial x} = a^2x. \tag{3.14}$$
- $$\frac{\partial u}{\partial y} = ax\sqrt{\frac{a}{\nu}}f''(\eta),$$

$$\begin{aligned}\frac{\partial^2 u}{\partial y^2} &= ax\sqrt{\frac{a}{\nu}}\frac{\partial}{\partial y}\big(f''(\eta)\big)\\ &= ax\sqrt{\frac{a}{\nu}}\big(\frac{\partial f''(\eta)}{\partial \eta}\frac{\partial \eta}{\partial y}\big)\\ &= ax\sqrt{\frac{a}{\nu}}\sqrt{\frac{a}{\nu}}\big(f'''(\eta)\big)\\ &= \frac{a^2 x}{\nu}\big(f'''(\eta)\big),\\ \nu(1-n)\frac{\partial^2 u}{\partial y^2} &= \nu(1-n)\left(\frac{a^2 x}{\nu}f'''(\eta)\right)\\ &= a^2 x(1-n)f'''(\eta). \end{aligned} \tag{3.15}$$

- $$\begin{aligned}\sqrt{2}\nu n\Gamma\big(\frac{\partial u}{\partial y}\big)\big(\frac{\partial^2 u}{\partial y^2}\big) &= \left(\sqrt{2}\nu n\Gamma\frac{a^3x^2}{\nu}\sqrt{\frac{a}{\nu}}\big(f''f'''(\eta)\big)\right)\\ &= \left(\frac{\sqrt{2a}\Gamma U}{\sqrt{\nu}}a^2 xn\big(f''f'''(\eta)\big)\right)\\ &= a^2 xnW_e(f''f'''(\eta)). \end{aligned} \tag{3.16}$$

- $$\frac{\sigma B_0^2}{\rho}(U-u) = \frac{ax\sigma B_0^2}{\rho}\big(1-f'(\eta)\big). \tag{3.17}$$

Using (3.9)-(3.17), the dimensionless form of (3.5) can be written as:

$$\begin{aligned} & a^2x\left(-\left(\frac{\eta b}{2}f''(\eta)+bf'(\eta)\right)+(f'(\eta))^2-\big(ff''(\eta)\big)\right)\\ & = a^2x\left(-b+1+(1-n)f'''(\eta)+nW_e\big(f''f'''(\eta)\big)+\frac{\sigma B_0^2}{\rho a}\big(1-f'(\eta)\big)\right).\\ \Rightarrow\quad & -\left(\frac{\eta b}{2}f''(\eta)+bf'(\eta)\right)+(f'(\eta))^2-\big(ff''(\eta)\big) = -b+1+(1-n)f'''(\eta)\\ & +nW_e\big(f''f'''(\eta)\big)+M\big(1-f'(\eta)\big).\\ \Rightarrow\quad & (1-n)f'''(\eta)+nW_e\big(f''f'''(\eta)\big)+M\big(1-f'(\eta)\big)-b+1+\frac{\eta b}{2}f''(\eta)\\ & +bf'(\eta)-(f'(\eta))^2+\big(f''f'''(\eta)\big)=0.\\ \Rightarrow\quad & (1-n)f'''(\eta)+\left(f(\eta)+\frac{\eta b}{2}\right)f''(\eta)-\big(f'(\eta)\big)^2+b(f'(\eta)-1)\\ & +nW_e\big(f''f'''(\eta)\big)+M(1-f'(\eta))+1=0. \end{aligned}$$

Further, (3.4) has been transformed into the dimensionless form as following procedure has been followed:

- $$\begin{aligned}\frac{\partial T}{\partial t} &= \frac{\partial}{\partial t}\left(T_\infty + q_0 x\sqrt{\nu}\left(\sqrt{s+bt}\theta(\eta)\right)\right)\\ &= q_0 x\sqrt{\nu}\left(\frac{b}{2\sqrt{s+bt}}\theta(\eta) + \left(\frac{\partial\theta}{\partial\eta}\frac{\partial\eta}{\partial t}\right)\sqrt{s+bt}\right)\\ &= q_0 x\sqrt{\nu}\left(\frac{\sqrt{a}b}{2}\theta(\eta) - \theta'(\eta)\frac{\eta ab}{2}\sqrt{s+bt}\right)\\ &= q_0 x\sqrt{\nu}\left(\frac{\sqrt{a}b}{2}\theta(\eta) - \theta'(\eta)\frac{\eta b}{2(s+bt)}\sqrt{s+bt}\right)\\ &= q_0 x\sqrt{\nu}\left(\frac{\sqrt{a}b}{2}\theta(\eta) - \theta'(\eta)\frac{\eta b}{2\sqrt{s+bt}\sqrt{s+bt}}\sqrt{s+bt}\right)\\ &= q_0 x\sqrt{\nu}\left(\frac{\sqrt{a}b}{2}\theta(\eta) - \theta'(\eta)\frac{\sqrt{a}\eta b}{2}\right)\\ &= q_0 x\sqrt{a\nu}\left(\frac{b}{2}\theta(\eta) - \frac{\eta b}{2}\theta'(\eta)\right).\end{aligned} \tag{3.18}$$
- $$\begin{aligned}\frac{\partial T}{\partial x} &= q_0\sqrt{\frac{\nu}{a}}\frac{\partial}{\partial x}\left(x\ \theta(\eta)\right)\\ &= q_0\sqrt{\frac{\nu}{a}}\left(x\left(\frac{\partial\theta}{\partial\eta}\frac{\partial\eta}{\partial x}\right) + \theta(\eta)\right)\\ &= q_0\sqrt{\frac{\nu}{a}}\theta(\eta).\end{aligned}$$
- $$\begin{aligned}u\frac{\partial T}{\partial x} &= \left(axf'(\eta)\right)\left(q_0\sqrt{\frac{\nu}{a}}\theta(\eta)\right)\\ &= a\ q_0 x\sqrt{\frac{\nu}{a}}\left(f'\theta(\eta)\right)\\ &= q_0 x\sqrt{a\nu}\left(f'\theta(\eta)\right).\end{aligned} \tag{3.19}$$
- $$\begin{aligned}\frac{\partial T}{\partial y} &= q_0 x\sqrt{\frac{\nu}{a}}\frac{\partial}{\partial y}\left(\theta(\eta)\right)\\ &= q_0 x\sqrt{\frac{\nu}{a}}\left(\frac{\partial\theta}{\partial\eta}\frac{\partial\eta}{\partial y}\right)\\ &= q_0 x\sqrt{\frac{\nu}{a}}\sqrt{\frac{a}{\nu}}\theta'(\eta)\\ &= q_0 x\theta'(\eta).\end{aligned} \tag{3.20}$$
- $$\begin{aligned}v\frac{\partial T}{\partial y} &= -\left(\sqrt{a\nu}f(\eta)\right)\left(q_0 x\theta'(\eta)\right)\\ &= -q_0 x\sqrt{a\nu}(f\theta')(\eta).\end{aligned}$$

(3.21)

- $$\frac{\partial}{\partial y}\left(\alpha(t)\frac{\partial T}{\partial y}\right) = \frac{\partial}{\partial y}\left(\alpha_\infty(1+\epsilon\theta\frac{\partial T}{\partial y}\right)$$
$$= \left(\left(\alpha_\infty\epsilon\frac{\partial\theta(\eta)}{\partial\eta}\frac{\partial\eta}{\partial y}\right)\frac{\partial T}{\partial y} + \alpha_\infty(1+\epsilon\theta)\left(\frac{\partial^2 T}{\partial y^2}\right)\right)$$
$$= \left(\alpha_\infty\epsilon\theta'(\eta)\sqrt{\frac{a}{\nu}}q_0x\theta'(\eta) + \alpha_\infty(1+\epsilon\theta)q_0x\sqrt{\frac{a}{\nu}}\theta''(\eta)\right)$$
$$= q_0x\sqrt{\frac{a}{\nu}}\left(\alpha_\infty\epsilon(\theta'(\eta))^2 + \alpha_\infty(1+\epsilon\theta)\theta''(\eta)\right). \quad (3.22)$$

Using (3.18)-(3.22), (3.4) has been transformed into the dimensionless form as follows:

$$q_0x\sqrt{a\nu}\left(\left(\frac{b}{2}\theta(\eta) - \frac{\eta b}{2}\theta'(\eta)\right) + \big(f'\theta(\eta)\big) - \big(f\theta'(\eta)\big)\right)$$
$$= q_0x\sqrt{\frac{a}{\nu}}\left(\alpha_\infty\epsilon\ (\theta'(\eta))^2 + \alpha_\infty\ (1+\epsilon\theta)\theta''(\eta)\right).$$
$$\Rightarrow \quad \sqrt{a\nu}\left(\left(\frac{b}{2}\theta(\eta) - \frac{\eta b}{2}\theta'(\eta)\right) + \big(f'\theta(\eta)\big) - \big(f\theta'(\eta)\big)\right)$$
$$= \sqrt{\frac{a}{\nu}}\left(\alpha_\infty\epsilon\ (\theta'(\eta))^2 + \alpha_\infty\ (1+\epsilon\theta)\theta''(\eta)\right).$$
$$\Rightarrow \quad \left(\left(\frac{b}{2}\theta(\eta) - \frac{\eta b}{2}\theta'(\eta)\right) + \big(f'\theta(\eta)\big) - \big(f\theta'(\eta)\big)\right)$$
$$= \frac{\alpha_\infty}{\nu}\left(\epsilon\ (\theta'(\eta))^2 + (1+\epsilon\theta)\theta''(\eta)\right).$$
$$\Rightarrow \quad \left(\left(\frac{b}{2}\theta(\eta) - \frac{\eta b}{2}\theta'(\eta)\right) + \big(f'\theta(\eta)\big) - \big(f\theta'(\eta)\big)\right)$$
$$= \frac{1}{Pr}\left(\epsilon\ \big(\theta'(\eta)\big)^2 + (1+\epsilon\theta)\theta''(\eta)\right).$$
$$\Rightarrow \quad Pr\left(\left(\frac{b}{2}\theta(\eta) - \frac{\eta b}{2}\theta'(\eta)\right) + \big(f'\theta(\eta)\big) - \big(f\theta'(\eta)\big)\right)$$
$$= \left(\epsilon\ (\theta'(\eta))^2 + (1+\epsilon\theta)\theta''(\eta)\right).$$
$$\Rightarrow \quad (1+\epsilon\theta)\theta''(\eta) + Pr\left(f(\eta) + \frac{b\eta}{2}\right)\theta'(\eta) + \epsilon\big(\theta'(\eta)\big)^2$$
$$- Pr\left(f'(\eta) + \frac{b}{2}\right)\theta(\eta) = 0.$$

The dimensionless form of the (3.6) by using the transformations (3.7) as follows.

- $u(x,y,t) = 0$ at $y = 0$

  $\Rightarrow$ $axf'(\eta) = 0$ at $\eta = 0$

  $\Rightarrow$ $f'(0) = 0.$

- $v(x,y,t) = \nu_0(t)$ at $y = 0$

  $\Rightarrow$ $-\sqrt{a\nu}f(\eta) = \nu_0(t)$ at $\eta = 0$

  $\Rightarrow$ $f(0) = -\dfrac{\nu_0(t)}{\sqrt{a\nu}} = -\dfrac{\nu\sqrt{a}}{\sqrt{a\nu}} = -\sqrt{\nu} = -f_0.$

- $-k\dfrac{\partial T(x,y,t)}{\partial y} = kq_0x$ at $y = 0$

  $\Rightarrow$ $-kq_0x\theta'(\eta) = kq_0x$ at $\eta = 0$

  $\Rightarrow$ $\theta'(0) = -1.$

- $u(x,y,t) \to U(x,t) = ax$ as $y \to \infty$

  $\Rightarrow$ $axf'(\eta) \to ax$ as $\eta \to \infty$

  $\Rightarrow$ $f'(\eta) \to 1.$ as $\eta \to \infty$

- $T(x,y,t) \to T_\infty$ as $y \to \infty$

  $\Rightarrow$ $T_\infty + \theta(\eta)q_0x\sqrt{\dfrac{\nu}{a}} \to T_\infty$ as $\eta \to \infty$

  $\Rightarrow$ $\theta(\eta) \to 0$ as $\eta \to \infty$

The final dimensionless form of the mathematical model describing the flow can, now, be concluded as:

$$\left.\begin{aligned}
&(1-n)f'''(\eta) + \left(f(\eta) + \frac{\eta b}{2}\right)f''(\eta) - \big(f'(\eta)\big)^2 + b(f'(\eta) - 1)\\
&+ nW_e\big(f''f'''(\eta)\big) + M(1 - f'(\eta)) + 1 = 0,\\
&(1+\epsilon\theta)\theta''(\eta) + Pr\left(f(\eta) + \frac{b\eta}{2}\right)\theta'(\eta) + \epsilon\big(\theta'(\eta)\big)^2\\
&- Pr\left(f'(\eta) + \frac{b}{2}\right)\theta(\eta) = 0,
\end{aligned}\right\} \tag{3.23}$$

subject to the following boundary values:

$$\left.\begin{aligned} &f(0) = -f_0, \quad f'(0) = 0, \quad \theta'(0) = -1, \qquad \eta = 0. \\ &f'(\infty) \to 1, \quad \theta(\infty) \to 0, \qquad\qquad\quad \eta \to \infty. \end{aligned}\right\} \tag{3.24}$$

The Weissenberg number W_e, magnetic parameter M and Prandtl number Pr are formulated as $W_e = \frac{\sqrt{2a}\Gamma U}{\sqrt{\nu}}$, $M = \frac{\sigma B_0^2}{\rho a}$, $Pr = \frac{\nu}{\alpha_\infty}$.

3.4 Numerical Treatment

The coupled ODEs (3.23) with the boundary values (3.24) have been solved by the well know shooting technique. The above ODEs can be re-written as:

$$f''' = \frac{1}{1-n+nW_e f''}\left((f')^2 - \left(f + \frac{\eta b}{2}\right)f'' - b(f'-1) - M(1-f') - 1\right) = 0, \tag{3.25}$$

$$\theta'' = \frac{1}{1+\epsilon\theta}\left(Pr\left(f' + \frac{b}{2}\right)\theta - Pr\left(f + \frac{b\eta}{2}\right)\theta' - \epsilon(\theta')^2\right). \tag{3.26}$$

By using following notations:

$$f = y_1, \quad f' = y_2, \quad f'' = y_3, \quad \theta = y_4, \quad \theta' = y_5,$$

To implement the RK-4 method on the above scheme of first order ODEs, the missing initial values $w = w_0$ and $z = z_0$ are to be chosen by hit and trial. For the refinement of the missing initial values by the Newton's method, the following notations have been introduced.

$$\begin{aligned} &\frac{\partial y_1}{\partial w} = y_6, \quad \frac{\partial y_2}{\partial w} = y_7, \quad \frac{\partial y_3}{\partial w} = y_8, \quad \frac{\partial y_4}{\partial w} = y_9, \quad \frac{\partial y_5}{\partial w} = y_{10}, \\ &\frac{\partial y_1}{\partial z} = y_{11}, \quad \frac{\partial y_2}{\partial z} = y_{12}, \quad \frac{\partial y_3}{\partial z} = y_{13}, \quad \frac{\partial y_4}{\partial z} = y_{14}, \quad \frac{\partial y_5}{\partial z} = y_{15}. \end{aligned}$$

Differentiating each of the first order ODEs of the above system, first w.r.t. w and then w.r.t. z, we get the following IVP is obtained.

$$y_1' = y_2, \qquad y_1(0) = -f_0,$$

$$y_2' = y_3, \qquad y_2(0) = 0,$$

$$y_3' = \frac{1}{1-n+nW_e y_3}\Bigg[(y_2)^2 - \left(y_1 y_3 + \frac{\eta b}{2} y_3\right) - b(y_2 - 1) - M(1 - y_2) - 1\Bigg], \qquad y_3(0) = w,$$

$$y_4' = y_5, \qquad y_4(0) = z,$$

$$y_5' = \frac{1}{1+\epsilon y_4}\left[Pr\left(y_2 y_4 + \frac{b}{2} y_4\right) - Pr\left(y_1 y_5 + \frac{\eta b}{2} y_5\right) - \epsilon (y_5)^2\right], \qquad y_5(0) = -1,$$

$$y_6' = y_7, \qquad y_6(0) = 0,$$

$$y_7' = y_8, \qquad y_7(0) = 0,$$

$$y_8' = \frac{1}{(1-n+nW_e y_3)^2}\Bigg[\Bigg(2(y_2 y_7) - \left(y_1 y_8 + y_3 y_6 + \frac{b\eta}{2} y_8\right) - b y_7 + M y_7\Bigg)\big(1 - n + nW_e y_3\big) - nW_e y_8\Bigg((y_2)^2 - \left(y_1 y_3 + \frac{b\eta}{2} y_3\right) - b(y_2 - 1) - M(1 - y_2) - 1\Bigg)\Bigg], \qquad y_8(0) = 1,$$

$$y_9' = y_{10}, \qquad y_9(0) = 0,$$

$$y_{10}' = \frac{1}{(1+\epsilon y_4)^2}\Bigg[\Bigg(Pr\left(y_2 y_9 + y_4 y_7 + \frac{b}{2} y_9\right) - Pr\Bigg(y_1 y_{10} + y_5 y_6 + \frac{b\eta}{2} y_{10}\Bigg) - 2\epsilon y_5 y_{10}\Bigg)\big(1 + \epsilon y_4\big) - \epsilon y_9\Bigg(Pr\left(y_2 y_4 + \frac{b}{2} y_4\right) - Pr\left(y_1 y_5 + \frac{b\eta}{2} y_5\right) - \epsilon y_5^2\Bigg)\Bigg], \qquad y_{10}(0) = 0,$$

$$y_{11}' = y_{12}, \qquad y_{11}(0) = 0,$$

$$y_{12}' = y_{13}, \qquad y_{12}(0) = 0,$$

$$y_{13}' = \frac{1}{(1-n+nW_e y_3)^2}\Bigg[\Bigg(2(y_2 y_{12}) - \left(y_1 y_{13} + y_3 y_{11} + \frac{b\eta}{2} y_{13}\right) - b y_{12} + M y_{12}\Bigg)\left(1 - n + nW_e y_3\right) - nW_e y_{13}\Bigg((y_2)^2 - \left(y_1 y_3 + \frac{b\eta}{2} y_3\right) - b(y_2 - 1) - M(1 - y_2) - 1\Bigg)\Bigg], \qquad y_{13}(0) = 0,$$

$$y_{14}' = y_{15}, \qquad y_{14}(0) = 1,$$

$$y_{15}' = \frac{1}{(1+\epsilon y_4)^2}\Bigg[\Bigg(Pr\left(y_2 y_{14} + y_4 y_{12} + \frac{b}{2} y_{14}\right) - Pr\Bigg(y_1 y_{15} + y_5 y_{11} + \frac{b\eta}{2} y_{15}\Bigg) - 2\epsilon y_5 y_{15}\Bigg)\big(1 + \epsilon y_4\big) - \epsilon y_{14}\Bigg(Pr\left(y_2 y_4 + \frac{b}{2} y_4\right) - Pr\left(y_1 y_5 + \frac{b\eta}{2} y_5\right) - \epsilon y_5^2\Bigg)\Bigg]. \qquad y_{15}(0) = 0,$$

It is important to mention that for an approximate solution, the unbounded domain $[0,\ \infty)$ has to be replaced by a bounded domain $[0,\ \eta_{max}]$ in such a way that the variation in the solution for $\eta > \eta_{max}$ is negligible. On the basis of observations, η_{max} has been chosen as 5 for the present work. The missing conditions w and z are iteratively updated by the Newton's technique as follows.

$$\begin{bmatrix} w^{n+1} \\ z^{n+1} \end{bmatrix} = \begin{bmatrix} w^{n} \\ z^{n} \end{bmatrix} - \begin{bmatrix} y_8(w^n, z^n) & y_{13}(w^n, z^n) \\ y_9(w^n, z^n) & y_{14}(w^n, z^n) \end{bmatrix}^{-1}_{\eta=\eta_{max}} \begin{bmatrix} y_2(w^n, z^n) - 1 \\ y_4(w^n, z^n) \end{bmatrix}_{\eta=\eta_{max}}.$$

The stopping criteria for the iterative procedure has been ready as:

$$max\left\{\left|y_2(\eta_{max}-1)\right|, \left|y_4(\eta_{max})\right|\right\} < \zeta,$$

where ζ is a sufficiently small +ve number. For the computations presented in this thesis, ζ has been taken as 10^{-6}. The choice of missing initial conditions is a crucial part of the numerical procedure. In Table 3.1, the intervals $[w_i \quad w_f]$ and $[z_i \quad z_f]$ have been presented where from the missing initial conditions w_0 and z_0 can respectively be chosen.

f_0	ϵ	Pr	We	b	M	n	$[w_i$	$w_f]$	$[z_i$	$z_f]$
-0.2	0.1	1	0.1	0.1	1	0.2	[1.56	01.9]	[01.1,	1.74]
-0.3							[01.6	2.49]	[01.1	2.29]
-0.4							[1.20	1.50]	[1.09	2.79]
-0.1	0.0						[1.22	2.70]	[0.89	1.13]
	0.2						[1.57	2.59]	[1.05	1.44]
	0.3						[2.37	2.64]	[01.1	1.15]
	0.1	1.5					[1.49	2.26]	[0.94	1.11]
		2.0					[01.5	2.00]	[0.90	1.18]
		2.5					[1.56	1.90]	[0.88	1.18]
		1	0.5				[1.44	2.93]	[0.92	1.18]
			1				[01.1	3.37]	[0.85	1.19]
			1.5				[1.38	3.68]	[0.81	1.19]
			0.1	0.2			[1.46	2.39]	[0.99	1.20]
				0.4			[1.22	2.21]	[0.96	1.20]
				0.6			[1.11	2.04]	[0.93	1.20]
				0.1	0.1		[1.01	2.65]	[0.95	1.20]
					0.4		[1.19	2.58]	[0.97	1.20]
					0.8		[1.48	2.49]	[0.99	1.20]
					1	0.1	[1.39	2.44]	[1.01	1.20]
						0.4	[1.75	2.53]	[1.01	1.20]
						0.6	[2.00	2.61]	[1.01	1.20]

TABLE 3.1: The intervals for the choice of two missing conditions

.

3.5 Numerical Discussion

In the present section, effects of different physical parameters on the skin friction coefficient and local Nusselt number profiles have been presented and analysed.

3.5.1 Skin Friction and Nusselt Number

Table 3.2 illustrates the numerical results of skin friction C_f and Nusselt number Nu_x profiles under the impact of different physical quantities. It is investigated that the effect of skin friction decreases by increasing the physical parameters of squeezed flow index and n power-law index parameters. However, the skin friction behaviour is increasing as an increasing values of the permeable velocity, Pr express prandtl number, M magnetic parameter and W_e Weissenberg number parameters. The Nusselt number has an increasing trend for, the squeezed parameter b, M magnetic parameter, n power-law index and f_0 permeable velocity. The Weissenberg number W_e tend to decline the Nusselt number.

f_0	ϵ	Pr	We	b	M	n	$C_f\sqrt{\mathrm{Re}_x}$	$Nu_x\sqrt{\mathrm{Re}_x}$
-0.2	0.1	1	0.5	0.1	0.1	0.2	1.242333	-1.080632
-0.3							1.305357	-1.009713
-0.4							1.370198	-0.945697
-0.1	0.0						1.181204	-1.081391
	0.2						1.181204	-1.242778
	0.3						1.181204	-1.331331
	0.1	0.5					1.181204	-1.589973
		1.5					1.181204	-0.944823
		2					1.181204	-0.846303
		1	1				1.209229	-1.168998
			1.5				1.235042	-1.177645
			2				1.259079	-1.185504
			0.5	0.0			1.229456	-1.201291
				0.2			1.130937	-1.121644
				0.3			1.078362	-1.087658
				0.1	0.2		1.218494	-1.153168
					0.3		1.254744	-1.147382
					0.4		1.290037	-1.141941
					0.1	0.0	1.279091	-1.178891
						0.4	1.079515	-1.138835
						0.6	0.974302	-1.117447

TABLE 3.2: Numerical results for skin friction, Nusselt number

3.5.2 Effect of Weissenberg Number

Figure 3.2 shows the behaviour of the velocity profile due to the increasing values of Weissenberg number W_e, which is the ratio of the relaxation time to the processing time. If the Weissenberg number increase, the fluid offers more resistance which reduces the velocity. Figure 3.3 presents the temperature profile under the impact of Weissenberg number. The temperature profile can be seen to be influenced in the increasing sense.

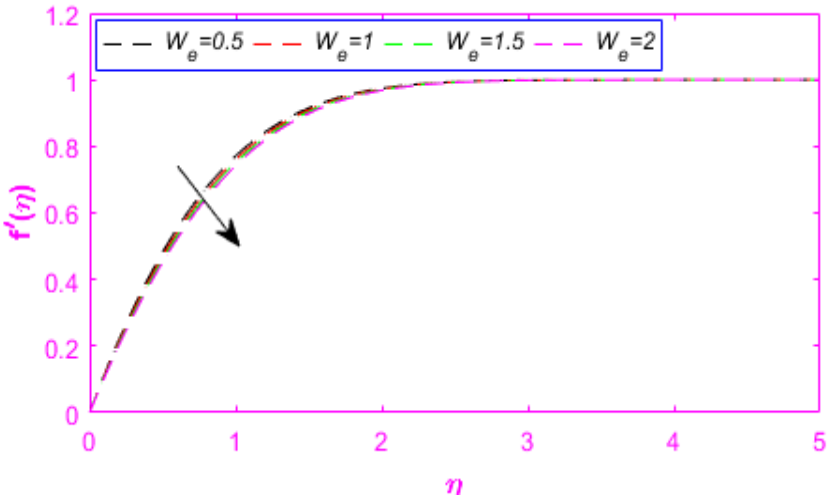

FIGURE 3.2: Variation of Weissenberg number.

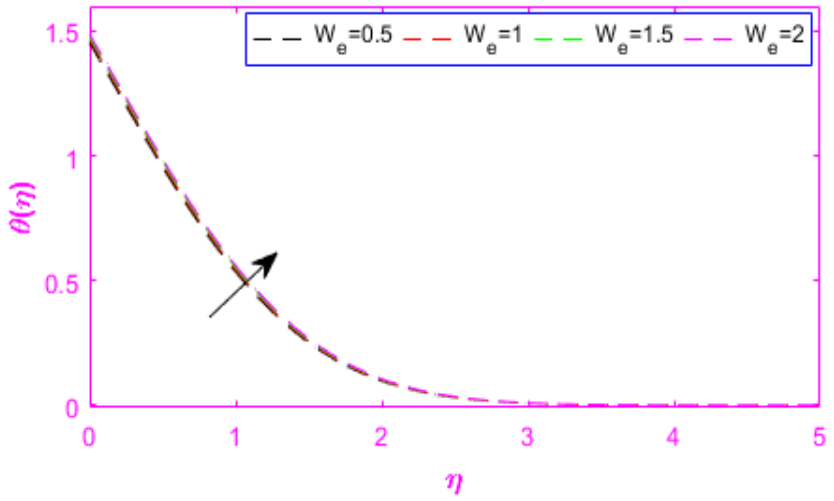

FIGURE 3.3: Variation of Weissenberg number.

3.5.3 Impact of Squeezed Flow Index

Figure 3.4 depict the behaviour of the velocity profile under the impact of the squeezing flow index b. If the squeezing index is increased, the fluid's velocity is observed to decrease. When the squeezing flow index b is increased, the strength of squeeze is decreased which declines the kinetic energy. As a result the velocity bears a reduction. In case of temperature profile, the effect of the squeezing flow index is shown in Figure 3.5 . It is observed that by increasing the values of the squeezing flow index, the thermal boundary layer thickness is decreased.

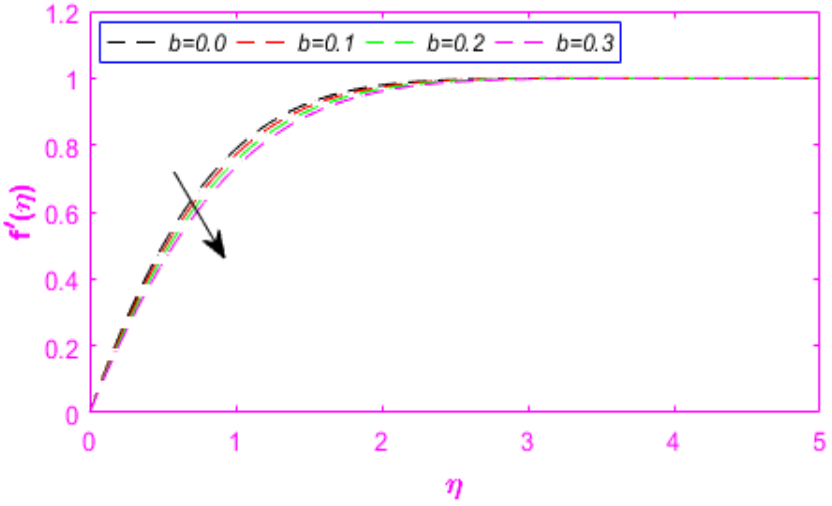

FIGURE 3.4: Variation of squeezed flow index.

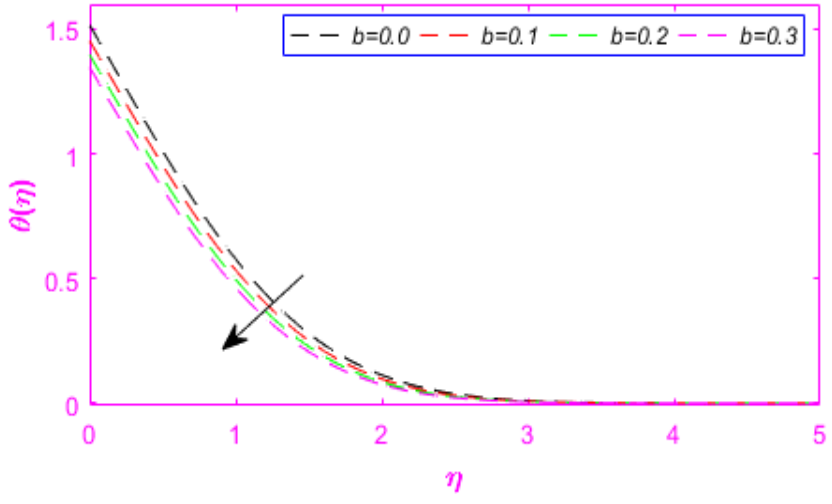

FIGURE 3.5: Variation of squeezed flow index.

3.5.4 Effect of Magnetic Parameter

To show the effect of the magnetic parameter M on the velocity profile will be analyse in the following discussion. In Figure 3.6, it is shown that if we increase the magnetic number, the velocity profile also increases. When the magnetic number gets larger values, the fluid is normally assumed to be slowed down. However, Figure 3.6 reflects an opposite behaviour. It is due to the squeezing phenomenon which has more stronger effect than the magnetic field. In case of temperature profile, when we increases of the magnetic number, a decreasing trend can be noticed in Figure 3.7.

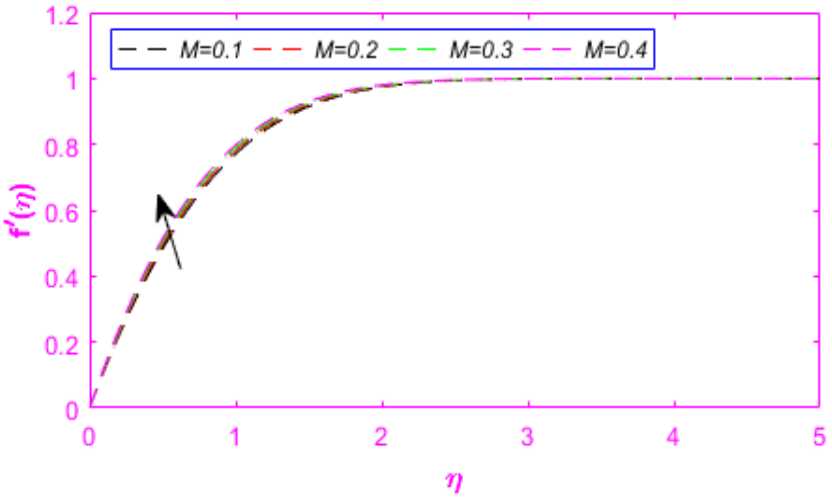

FIGURE 3.6: Variation of magnetic number.

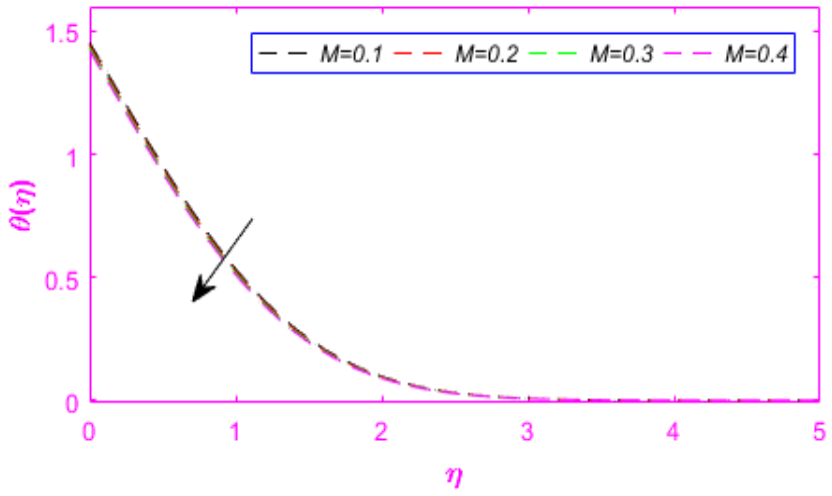

FIGURE 3.7: Variation of magnetic number.

3.5.5 Effect of Power Law Index

To show the impact of the power-law index n on the velocity and temperature profiles, Figures 3.8 and 3.9 have been included. A increasing the velocity of fluid and decreasing the temperature behaviour can be observed due to the shear thinning effect its viscosity decreases with shear strain.

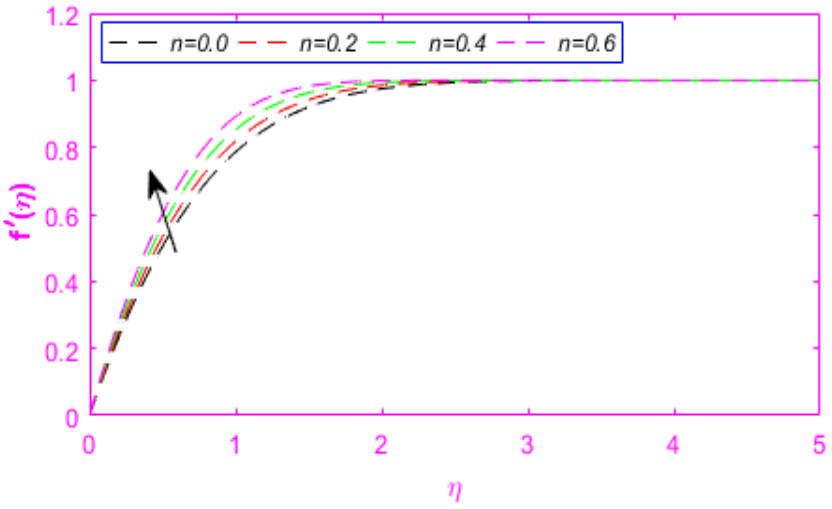

FIGURE 3.8: Variation of power-law index.

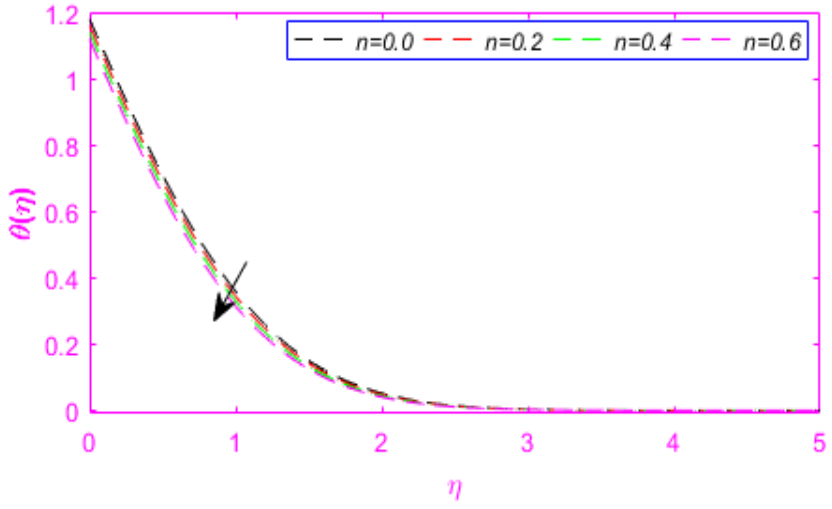

FIGURE 3.9: Variation of power-law index.

3.5.6 Effect of Permeable Velocity

Figures 3.10 and 3.11 shows the permeable velocity behaviour on the velocity and temperature profiles. The velocity profile can be seen to increase if the permeable velocity f_0 bears an increment for the suction case. This behaviour happens due to the fact that suction is responsible for pushing the fluid towards the sensor surface. The permeable velocity leaves a similar effect on the temperature distribution as presented in Figure 3.11.

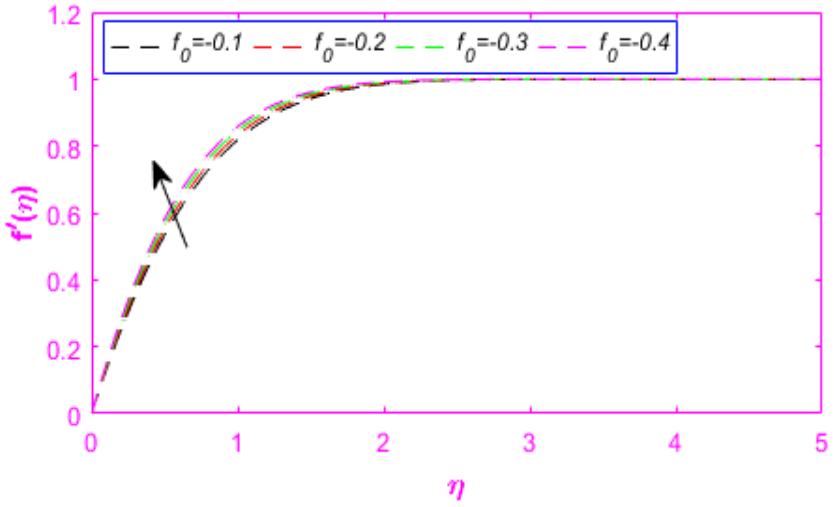

FIGURE 3.10: Variation of permeable velocity.

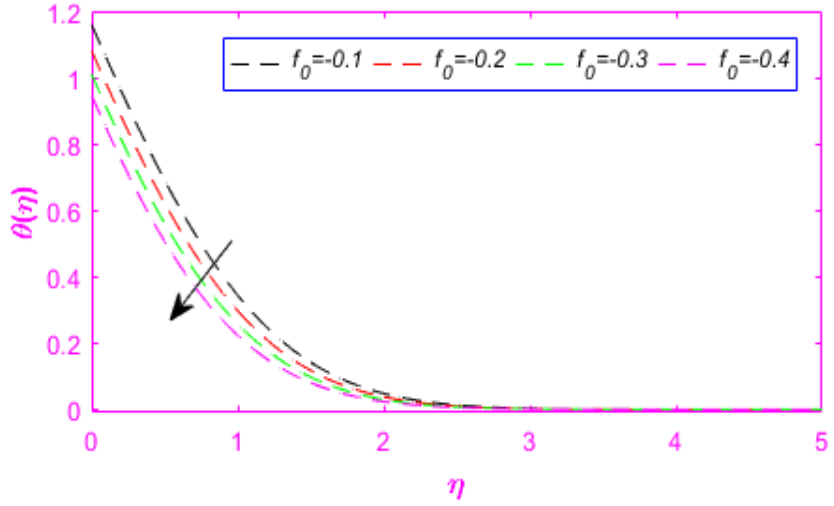

FIGURE 3.11: Variation of permeable velocity.

3.5.7 Effect of Prandtl Number and ϵ

Figure 3.12 indicates the impact of Prandtl number Pr on the temperature. Prandtl number as defined by the ratio of momentum diffusivity to the thermal diffusivity. The temperature behaviour decrease for the increasing values of the prandtl number. Figure 3.13 shows an increasing behaviour of the temperature profile for increasing values of ϵ. It happens because for higher values of ϵ, the kinetic energy gets larger which causes the temperature to rise.

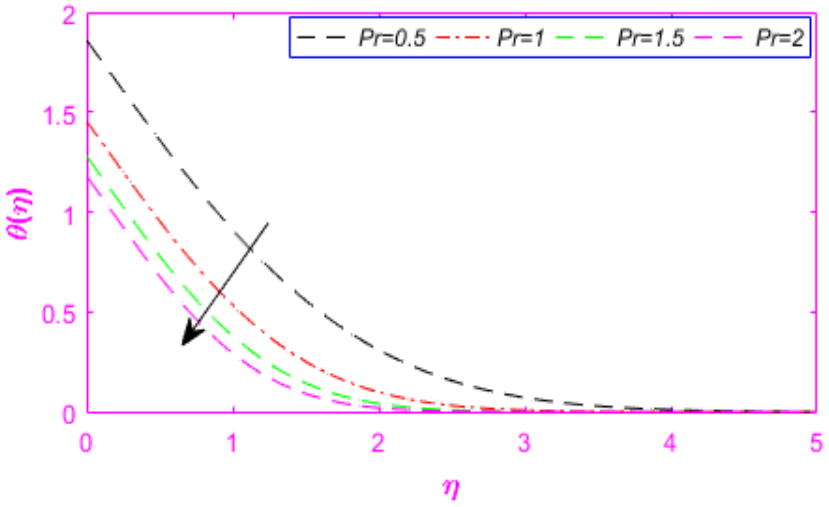

FIGURE 3.12: Variation of Prandtl number.

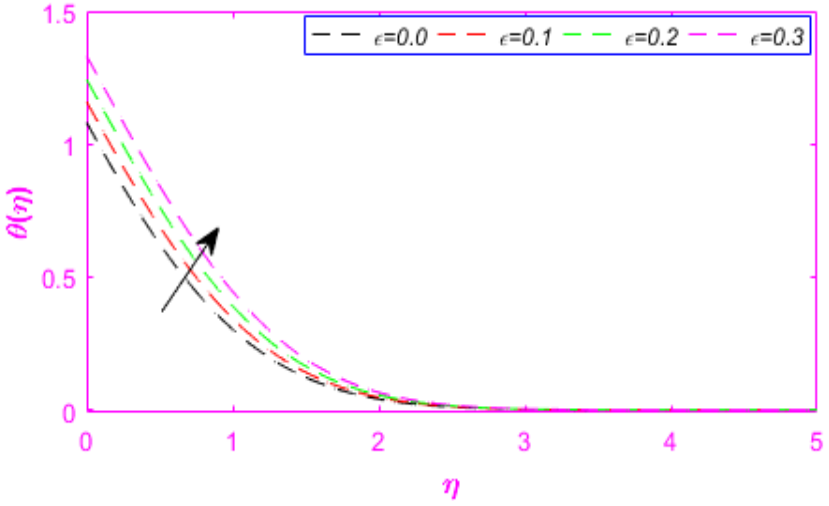

FIGURE 3.13: Variation of small parameter.

Chapter 4

Squeezing Flow of Tangent Hyperbolic Fluid over a Sensor Plate

4.1 Introduction

In this chapter, we have extended the work of Kumar et al. [24]. In the present work, the squeezing flow model is modified by including the effect of variable thermal radiation of a tangent hyperbolic fluid towards a sensor plate. Further, the modified non-dimensional energy equation are reduced into the dimensionless form by using the applicable transformations. The numerical results is access by shooting technique scripted in the computational software Matlab. The numerical results of skin friction, Nusselt number and profiles of physical interest are analysed through tables and graphs for different physical parameters.

4.2 Mathematical Model

Consider a flow with the same geometry as shown in Figure 3.1. In addition to all the assumptions described in Chapter 3, the effect of thermal radiation has been incorporated in the present model. As a result of inclusion of this physical phenomena, only the energy equation will be updated. The modified version of the partial differential equation (3.4) has been presented below.

$$\begin{aligned}\frac{\partial u}{\partial t}+u\frac{\partial u}{\partial x}+v\frac{\partial u}{\partial y}&=\frac{\partial U}{\partial t}+U\frac{\partial U}{\partial x}\\&\quad+\nu(1-n)\frac{\partial^2 u}{\partial y^2}+\sqrt{2}\nu n\Gamma\left(\frac{\partial u}{\partial y}\right)\frac{\partial^2 u}{\partial y^2}+\frac{\sigma B_0^2}{\rho}(U-u).\end{aligned}\tag{4.1}$$

$$\frac{\partial T}{\partial t}+u\frac{\partial T}{\partial x}+v\frac{\partial T}{\partial y}=\frac{\partial}{\partial y}\left(\alpha(T)\frac{\partial T}{\partial y}\right)-\frac{1}{\rho C_p}\frac{\partial q_r}{\partial y}.\tag{4.2}$$

The boundary values are given below:

$$\left.\begin{aligned}&y=0,\ u(x,y,t)=0,\ v(x,y,t)=\nu_0(t),\ -k\frac{\partial T(x,y,t)}{\partial y}=kq(x),\\&y\to\infty,\ u(x,y,t)\to U(x,t),\ T(x,y,t)\to T_\infty.\end{aligned}\right\}\tag{4.3}$$

4.3 Transformation

The modified governing equation (4.2) are reduced into the dimensionless form by using the following applicable transformations:

$$\left.\begin{aligned}&U=ax,\ \psi=\sqrt{a\nu}xf(\eta),\ a=\frac{1}{s+bt},\ u=axf'(\eta),\ v=-\sqrt{a\nu}f(\eta),\\&T=T_\infty+\theta(\eta)q_0x\sqrt{\frac{\nu}{a}},\ \eta=y\sqrt{\frac{a}{\nu}}=y\sqrt{\frac{1}{\nu(s+bt)}}.\end{aligned}\right\}\tag{4.4}$$

In the above transformations, U the free stream velocity, a the strength of squeezing flow, b the squeezing flow index, s an arbitrary constant, $q_0(x)$ the heat flux, T express temperature, T_∞ present free stream temperature and ψ stream function.

The radiation approximated by the Rosseland approach is

$$q_r = -\frac{4\sigma^*}{3k^*}\frac{\partial T^4}{\partial y}. \tag{4.5}$$

Here k^* the absorption coefficient and σ^* Stefan-Boltzmann constant. By applying Taylor series for free stream temperature and ignoring the higher order terms.

- $$T^4 = 4T_\infty^3 T - 3T_\infty^4 \tag{4.6}$$

$$\Rightarrow \frac{\partial T^4}{\partial y} = 4T_\infty^3 \frac{\partial T}{\partial y} \tag{4.7}$$

Using (4.6) in (4.5), and further differentiate w.r.t. y, we get

$$\frac{\partial q_r}{\partial y} = -\frac{16\sigma^* T_\infty^3}{3k^*}\frac{\partial^2 T}{\partial y^2}. \tag{4.8}$$

We, now, convert the dimensional energy equation (4.2) with boundary conditions (4.3) into the dimensionless form by using the above similarity transformations.

- $$\begin{aligned}
\frac{\partial T}{\partial t} &= \frac{\partial}{\partial t}\left(T_\infty + q_0 x\sqrt{\nu}\left(\sqrt{s+bt}\theta(\eta)\right)\right) \\
&= q_0 x\sqrt{\nu}\left(\frac{b}{2\sqrt{s+bt}}\theta(\eta) + \left(\frac{\partial\theta}{\partial\eta}\frac{\partial\eta}{\partial t}\right)\sqrt{s+bt}\right) \\
&= q_0 x\sqrt{\nu}\left(\frac{\sqrt{a}b}{2}\theta(\eta) - \theta'(\eta)\frac{\eta ab}{2}\sqrt{s+bt}\right) \\
&= q_0 x\sqrt{\nu}\left(\frac{\sqrt{a}b}{2}\theta(\eta) - \theta'(\eta)\frac{\eta b}{2(s+bt)}\sqrt{s+bt}\right) \\
&= q_0 x\sqrt{\nu}\left(\frac{\sqrt{a}b}{2}\theta(\eta) - \theta'(\eta)\frac{\eta b}{2\sqrt{s+bt}\sqrt{s+bt}}\sqrt{s+bt}\right) \\
&= q_0 x\sqrt{\nu}\left(\frac{\sqrt{a}b}{2}\theta(\eta) - \theta'(\eta)\frac{\sqrt{a}\eta b}{2}\right) \\
&= q_0 x\sqrt{a\nu}\left(\frac{b}{2}\theta(\eta) - \frac{\eta b}{2}\theta'(\eta)\right).
\end{aligned} \tag{4.9}$$

- $$\frac{\partial T}{\partial x} = q_0\sqrt{\frac{\nu}{a}}\frac{\partial}{\partial x}\big(x\ \theta(\eta)\big)$$
$$= q_0\sqrt{\frac{\nu}{a}}\left(x\left(\frac{\partial\theta}{\partial\eta}\frac{\partial\eta}{\partial x}\right)+\theta(\eta)\right)$$
$$= q_0\sqrt{\frac{\nu}{a}}\theta(\eta). \tag{4.10}$$
- $$u\frac{\partial T}{\partial x} = \big(axf'(\eta)\big)\left(q_0\sqrt{\frac{\nu}{a}}\theta(\eta)\right)$$
$$= q_0x\ a\sqrt{\frac{\nu}{a}}\left(\big(f'\theta(\eta)\big)\right)$$
$$= q_0x\sqrt{a\nu}\big(f'\theta(\eta)\big). \tag{4.11}$$
- $$\frac{\partial T}{\partial y} = q_0x\sqrt{\frac{\nu}{a}}\frac{\partial}{\partial y}\left(\theta(\eta)\right)$$
$$= q_0x\sqrt{\frac{\nu}{a}}\left(\frac{\partial\theta}{\partial\eta}\frac{\partial\eta}{\partial y}\right)$$
$$= q_0x\sqrt{\frac{\nu}{a}}\sqrt{\frac{a}{\nu}}\theta'(\eta)$$
$$= q_0x\ \theta'(\eta). \tag{4.12}$$
- $$v\frac{\partial T}{\partial y} = -\big(\sqrt{a\nu}f(\eta)\big)\big(q_0x\theta'(\eta)\big)$$
$$= -q_0x\sqrt{a\nu}\big(f\theta'(\eta)\big). \tag{4.13}$$
- $$\frac{\partial}{\partial y}\left(\alpha(t)\frac{\partial T}{\partial y}\right) = \frac{\partial}{\partial y}\left(\alpha_\infty(1+\epsilon\theta\frac{\partial T}{\partial y}\right)$$
$$= \left(\left(\alpha_\infty\epsilon\frac{\partial\theta(\eta)}{\partial\eta}\frac{\partial\eta}{\partial y}\right)\frac{\partial T}{\partial y}+\alpha_\infty(1+\epsilon\theta)\left(\frac{\partial^2T}{\partial y^2}\right)\right)$$
$$= \left(\alpha_\infty\epsilon\theta'(\eta)\sqrt{\frac{a}{\nu}}q_0x\theta'(\eta)+\alpha_\infty(1+\epsilon\theta)q_0x\sqrt{\frac{a}{\nu}}\theta''(\eta)\right)$$
$$= q_0x\sqrt{\frac{a}{\nu}}\left(\alpha_\infty\epsilon(\theta'(\eta))^2+\alpha_\infty(1+\epsilon\theta)\theta''(\eta)\right). \tag{4.14}$$
- $$\frac{\partial q_r}{\partial y} = -\frac{16\sigma^*T_\infty^3}{3k^*}\left(\frac{\partial^2T}{\partial y^2}\right)$$
$$= -\frac{16\sigma^*T_\infty^3}{3k^*}\ q_0x\sqrt{\frac{a}{\nu}}\theta''(\eta).$$

$$\begin{aligned}\frac{1}{\rho C_p}\frac{\partial q_r}{\partial y} &= -\frac{16\sigma^* T_\infty^3}{3k^*\rho C_p}\, q_0 x\sqrt{\frac{a}{\nu}}\theta''(\eta)\\ &= -\left(\frac{4\sigma^* T_\infty^3}{k^* k}\right)\frac{4k}{3\rho C_p} q_0 x\sqrt{\frac{a}{\nu}}\theta''(\eta)\\ &= -\frac{4}{3}\left(\frac{k}{\rho C_p}\right) Rd\; q_0 x\sqrt{\frac{a}{\nu}}\theta''(\eta)\\ &= -\frac{4}{3} Rd\; \alpha_\infty q_0 x\sqrt{\frac{a}{\nu}}\theta''(\eta). \end{aligned} \tag{4.15}$$

Using (4.9)-(4.15), the energy equation (4.2) has been transformation into the dimensionless form as following procedure has been followed:

$$\begin{aligned} & q_0 x\sqrt{a\nu}\left(\left(\frac{b}{2}\theta(\eta) - \frac{\eta b}{2}\theta'(\eta)\right) + \big(f'\theta(\eta)\big) - \big(f\theta'(\eta)\big)\right)\\ &= q_0 x\sqrt{\frac{a}{\nu}}\left(\alpha_\infty\epsilon\,(\theta'(\eta))^2 + \alpha_\infty\,(1+\epsilon\theta)\theta''(\eta) + \frac{4}{3}Rd\;\alpha_\infty\theta''(\eta)\right).\\ \Rightarrow\quad & \sqrt{a\nu}\left(\left(\frac{b}{2}\theta(\eta) - \frac{\eta b}{2}\theta'(\eta)\right) + \big(f'\theta(\eta)\big) - \big(f\theta'(\eta)\big)\right)\\ &= \sqrt{\frac{a}{\nu}}\left(\alpha_\infty\epsilon\,(\theta'(\eta))^2 + \alpha_\infty\,(1+\epsilon\theta)\theta''(\eta) + \frac{4}{3}Rd\;\theta''(\eta)\right).\\ \Rightarrow\quad & \left(\left(\frac{b}{2}\theta(\eta) - \frac{\eta b}{2}\theta'(\eta)\right) + \big(f'\theta(\eta)\big) - \big(f\theta'(\eta)\big)\right)\\ &= \frac{\alpha_\infty}{\nu}\left(\epsilon\,(\theta'(\eta))^2 + (1+\epsilon\theta)\theta''(\eta) + \frac{4}{3}Rd\;\theta''(\eta)\right).\\ \Rightarrow\quad & \left(\left(\frac{b}{2}\theta(\eta) - \frac{\eta b}{2}\theta'(\eta)\right) + \big(f'\theta(\eta)\big) - \big(f\theta'(\eta)\big)\right)\\ &= \frac{1}{Pr}\left(\epsilon\,\big(\theta'(\eta)\big)^2 + (1+\epsilon\theta)\theta''(\eta) + \frac{4}{3}Rd\;\theta''(\eta)\right).\\ \Rightarrow\quad & Pr\left(\left(\frac{b}{2}\theta(\eta) - \frac{\eta b}{2}\theta'(\eta)\right) + \big(f'\theta(\eta)\big) - \big(f\theta'(\eta)\big)\right)\\ &= \left(\epsilon\,(\theta'(\eta))^2 + (1+\epsilon\theta)\theta''(\eta) + \frac{4}{3}Rd\;\theta''(\eta)\right).\\ \Rightarrow\quad & Pr\left(\left(\frac{b}{2}\theta(\eta) - \frac{\eta b}{2}\theta'(\eta)\right) + \big(f'\theta(\eta)\big) - \big(f\theta'(\eta)\big)\right)\\ &= \left(\epsilon\,(\theta'(\eta))^2 + (1+\epsilon\theta)\theta''(\eta) + \frac{4}{3}Rd\;\theta''(\eta)\right).\\ \Rightarrow\quad & (1+\epsilon\theta)\theta''(\eta) + Pr\left(f(\eta) + \frac{b\eta}{2}\right)\theta'(\eta) + \epsilon\big(\theta'(\eta)\big)^2\\ & - Pr\left(f'(\eta) + \frac{b}{2}\right)\theta(\eta) + \frac{4}{3}Rd\;\theta''(\eta) = 0. \end{aligned}$$

The final dimensionless form of the mathematical model describing the flow can, now, be concluded as:

$$\left.\begin{aligned}
&(1-n)f'''(\eta)+\left(f(\eta)+\frac{\eta b}{2}\right)f''(\eta)-\big(f'(\eta)\big)^2+b(f'(\eta)-1)\\
&+nW_e\big(f''f'''(\eta)\big)+M(1-f'(\eta))+1=0.\\
&(1+\epsilon\theta)\theta''(\eta)+Pr\left(f(\eta)+\frac{b\eta}{2}\right)\theta'(\eta)+\epsilon\big(\theta'(\eta)\big)^2\\
&-Pr\left(f'(\eta)+\frac{b}{2}\right)+\frac{4}{3}Rd\;\theta''(\eta)=0.
\end{aligned}\right\} \tag{4.16}$$

Subject to the following boundary values:

$$\left.\begin{aligned}
&f(0)=-f_0,\ f'(0)=0,\ \theta'(0)=-1,\ \eta=0.\\
&f'(\infty)\to 1,\ \theta(\infty)\to 0,\ \eta\to\infty.
\end{aligned}\right\} \tag{4.17}$$

The Weissenberg number W_e, magnetic field parameter M, Prandtl number Pr and Rd the thermal diffusivity are formulated as

$$W_e=\tfrac{\sqrt{2a}\Gamma U}{\sqrt{\nu}},\ M=\tfrac{\sigma B_0^2}{\rho a},\ Pr=\tfrac{\nu}{\alpha_\infty},\ Rd=\tfrac{4\sigma^* T_\infty^3}{k^* k}.$$

4.4 Numerical Treatment

The coupled non-linear ODEs (4.16) with the boundary values (4.17) have been computed by the shooting technique. The above ODEs can be re-written as:

$$f'''=\frac{1}{1-n+nW_e f''}\left((f')^2-\left(f+\frac{\eta b}{2}\right)f''-b(f'-1)-M(1-f')-1\right)=0, \tag{4.18}$$

$$\theta''=\frac{1}{1+\epsilon\theta+\frac{4}{3}Rd}\left(Pr\left(f'+\frac{b}{2}\right)\theta-Pr\left(f+\frac{b\eta}{2}\right)\theta'-\epsilon(\theta')^2\right). \tag{4.19}$$

By using following notations:

$$f=y_1,\quad f'=y_2,\quad f''=y_3,\quad \theta=y_4,\quad \theta'=y_5,$$

To implement the RK-4 method on the above scheme of first order ODEs, the missing initial values $w = w_0$ and $z = z_0$ are to be chosen by hit and trial. For the refinement of the missing initial values by the Newton's method, the following notations have been introduced.

$$\frac{\partial y_1}{\partial w} = y_6, \quad \frac{\partial y_2}{\partial w} = y_7, \quad \frac{\partial y_3}{\partial w} = y_8, \quad \frac{\partial y_4}{\partial w} = y_9, \quad \frac{\partial y_5}{\partial w} = y_{10},$$
$$\frac{\partial y_1}{\partial z} = y_{11}, \quad \frac{\partial y_2}{\partial z} = y_{12}, \quad \frac{\partial y_3}{\partial z} = y_{13}, \quad \frac{\partial y_4}{\partial z} = y_{14}, \quad \frac{\partial y_5}{\partial z} = y_{15}.$$

Differentiating each of the first order ODEs of the above system, first w.r.t. w and then w.r.t. z, we get the following IVP is obtained.

$$\begin{aligned}
y_1' &= y_2, && y_1(0) = -f_0,\\
y_2' &= y_3, && y_2(0) = 0,\\
y_3' &= \frac{1}{1-n+nW_e y_3}\Bigg[(y_2)^2 - \left(y_1 y_3 + \frac{\eta b}{2} y_3\right)\\
&\quad - b(y_2 - 1) - M(1 - y_2) - 1\Bigg], && y_3(0) = w,\\
y_4' &= y_5, && y_4(0) = z,\\
y_5' &= \frac{1}{1 + \epsilon y_4 + \frac{4}{3}Rd}\Bigg[Pr\left(y_2 y_4 + \frac{b}{2} y_4\right)\\
&\quad - Pr\left(y_1 y_5 + \frac{\eta b}{2} y_5\right) - \epsilon (y_5)^2\Bigg], && y_5(0) = -1,\\
y_6' &= y_7, && y_6(0) = 0,\\
y_7' &= y_8, && y_7(0) = 0,\\
y_8' &= \frac{1}{(1-n+nW_e y_3)^2}\Bigg[\Bigg(2(y_2 y_7) - \left(y_1 y_8 + y_3 y_6 + \frac{b\eta}{2} y_8\right)\\
&\quad - b y_7 + M y_7\Bigg)\big(1 - n + nW_e y_3\big) - nW_e y_8\Bigg((y_2)^2\\
&\quad - \left(y_1 y_3 + \frac{b\eta}{2} y_3\right) - b(y_2 - 1) - M(1 - y_2) - 1\Bigg)\Bigg], && y_8(0) = 1,
\end{aligned}$$

$$
\begin{aligned}
y_9' &= y_{10}, && y_9(0) = 0,\\
y_{10}' &= \frac{1}{(1+\epsilon y_4+\frac{4}{3}Rd)^2}\Bigg[\Bigg(Pr\Bigg(y_2y_9+y_4y_7+\frac{b}{2}y_9\Bigg)\\
&\quad - Pr\Bigg(y_1y_{10}+y_5y_6+\frac{b\eta}{2}y_{10}\Bigg)-2\epsilon y_5y_{10}\Bigg)\big(1+\epsilon y_4\big)\\
&\quad - \epsilon y_9\Bigg(Pr\Bigg(y_2y_4+\frac{b}{2}y_4\Bigg)-Pr\Bigg(y_1y_5+\frac{b\eta}{2}y_5\Bigg)-\epsilon y_5^2\Bigg)\Bigg], && y_{10}(0) = 0,\\
y_{11}' &= y_{12}, && y_{11}(0) = 0,\\
y_{12}' &= y_{13}, && y_{12}(0) = 0,\\
y_{13}' &= \frac{1}{(1-n+nW_ey_3)^2}\Bigg[\Bigg(2(y_2y_{12})-\Bigg(y_1y_{13}+y_3y_{11}+\frac{b\eta}{2}y_{13}\Bigg)\\
&\quad - by_{12}+My_{12}\Bigg)\Bigg(1-n+nW_ey_3\Bigg)-nW_ey_{13}\Bigg((y_2)^2\\
&\quad - \Bigg(y_1y_3+\frac{b\eta}{2}y_3\Bigg)-b(y_2-1)-M(1-y_2)-1\Bigg)\Bigg], && y_{13}(0) = 0,\\
y_{14}' &= y_{15}, && y_{14}(0) = 1,\\
y_{15}' &= \frac{1}{(1+\epsilon y_4+\frac{4}{3}Rd)^2}\Bigg[\Bigg(Pr\Bigg(y_2y_{14}+y_4y_{12}+\frac{b}{2}y_{14}\Bigg)\\
&\quad - Pr\Bigg(y_1y_{15}+y_5y_{11}+\frac{b\eta}{2}y_{15}\Bigg)-2\epsilon y_5y_{15}\Bigg)\big(1+\epsilon y_4\big)\\
&\quad - \epsilon y_{14}\Bigg(Pr\Bigg(y_2y_4+\frac{b}{2}y_4\Bigg)-Pr\Bigg(y_1y_5+\frac{b\eta}{2}y_5\Bigg)-\epsilon y_5^2\Bigg)\Bigg]. && y_{15}(0) = 0,
\end{aligned}
$$

As already done in Chapter 3, the unbounded domain $[0,\ \infty)$ has to be replaced by a bounded domain $[0,\ \eta_{max}]$ in such a way that the variation in the solution for $\eta > \eta_{max}$ is negligible. On the basis of observations, η_{max} has been chosen as 5 for the present work.

$$
\begin{bmatrix} w^{n+1} \\ z^{n+1} \end{bmatrix} = \begin{bmatrix} w^{n} \\ z^{n} \end{bmatrix} - \begin{bmatrix} y_8(w^n,z^n) & y_{13}(w^n,z^n) \\ y_9(w^n,z^n) & y_{14}(w^n,z^n) \end{bmatrix}^{-1}_{\eta=\eta_{max}} \begin{bmatrix} y_2(w^n,z^n)-1 \\ y_4(w^n,z^n) \end{bmatrix}_{\eta=\eta_{max}}.
$$

4.5 Numerical Discussion

In the present section, effects of different physical parameters on the Nusselt number profile have been presented and analysed.

4.5.1 Effect of Physical Parameters on Skin Friction and Nusselt Number

Table 4.1 illustrates the numerical results of the skin friction and Nusselt number under the impact of physical parameters. In order to shows that the effect of skin friction decreases by increasing physical parameters of b the squeezed flow index. However, the skin friction behaviour is increasing as an increasing values of the f_0 the permeable velocity, Pr the prandtl number, M the magnetic number and W_e Weissenberg number parameters. The Nusselt number has an increasing trend for, the squeezed parameter b, M the magnetic number and f_0 permeable velocity. The thermal radiation Rd tend to decline the Nusselt number.

f_0	ϵ	Pr	W_e	b	M	n	Rd	$C_f\sqrt{\mathrm{Re}_x}$	$Nu_x\sqrt{\mathrm{Re}_x}$
-0.2	0.1	1	0.5	0.1	0.1	0.2	1	1.242333	-3.599693
-0.3								1.305357	-3.445555
-0.4								1.370198	-3.301917
-0.1	0							1.181204	-3.660959
	0.2							1.181204	-3.927913
	0.3							1.181204	-4.097202
	0.1	0.5						1.181204	-5.107889
		1.5						1.181204	-3.152474
		2						1.181204	-2.780503
		1	1					1.209229	-3.791577
			1.5					1.235042	-3.815225
			2					1.259079	-3.836825
			0.5	0.0				1.229456	-3.880253
				0.2				1.130937	-3.661245
				0.3				1.078362	-3.566869
				0.1	0.2			1.218494	-3.748343
					0.3			1.254743	-3.732436
					0.4			1.290037	-3.717483
					0.1	0.0		1.279091	-3.822808
						0.4		1.079515	-3.704998
						0.6		0.974302	-3.642040
						0.2	0.5	1.181204	-2.355078
							1.5	1.181204	-5.351504
							2	1.181204	-7.087824

TABLE 4.1: Numerical results for skin friction, Nusselt number

4.5.2 Effect of Weissenberg Number

Figure 4.1 shows the behaviour of the velocity profile due to the increasing values of Weissenberg number W_e, which is the ratio of the relaxation time to the processing time. If the Weissenberg number increase, the fluid offers more resistance which reduces the velocity. Figure 4.2 illustrates the temperature profile under the impact of Weissenberg number. The temperature profile can be seen to be influenced in the increasing sense.

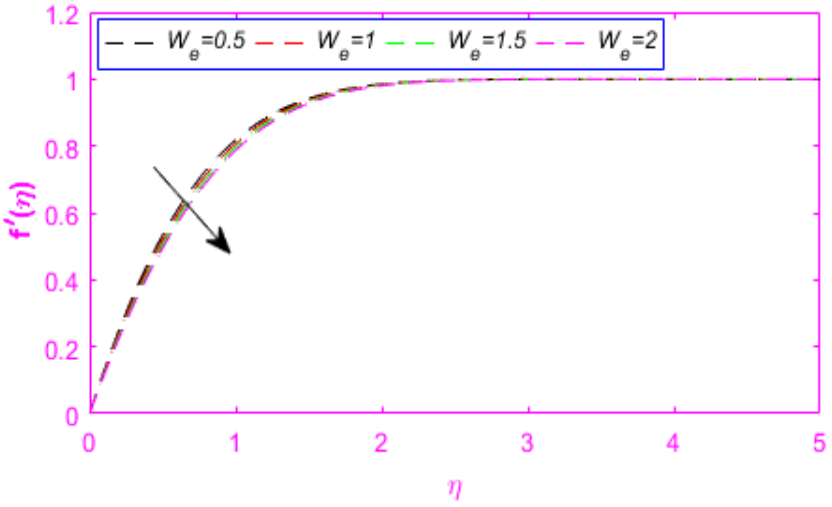

FIGURE 4.1: Variation of Weissenberg number.

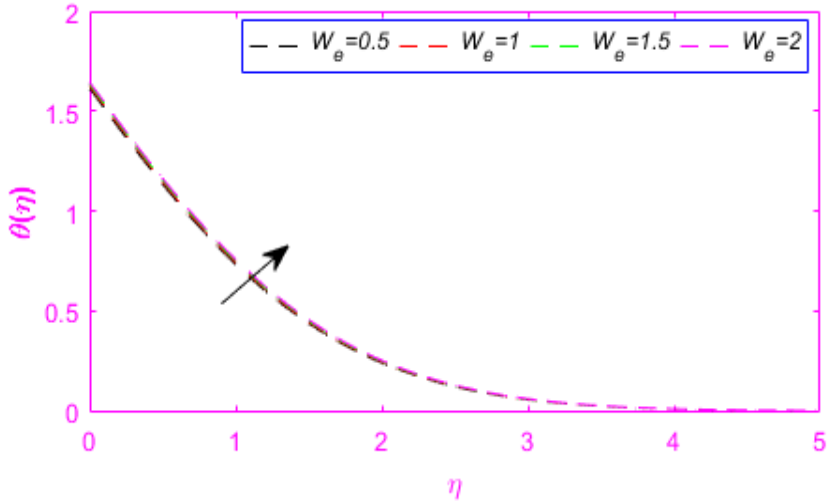

FIGURE 4.2: Variation of Weissenberg number.

4.5.3 Effect of Squeezed Flow Index

Figure 4.3 shows the behaviour of the velocity profile under the impact of the squeezing flow index b. If the squeezing flow index is increased, the fluid's velocity is observed to decrease. When the squeezing flow index b is increased, the strength of squeeze is decreased which declines the kinetic energy. As a result the velocity bears a reduction. In case of temperature profile, the effect of the squeezing flow index is shown in Figure 4.4 . It is observed that by increasing the squeezing flow index, the thermal boundary layer thickness of fluid is decreased.

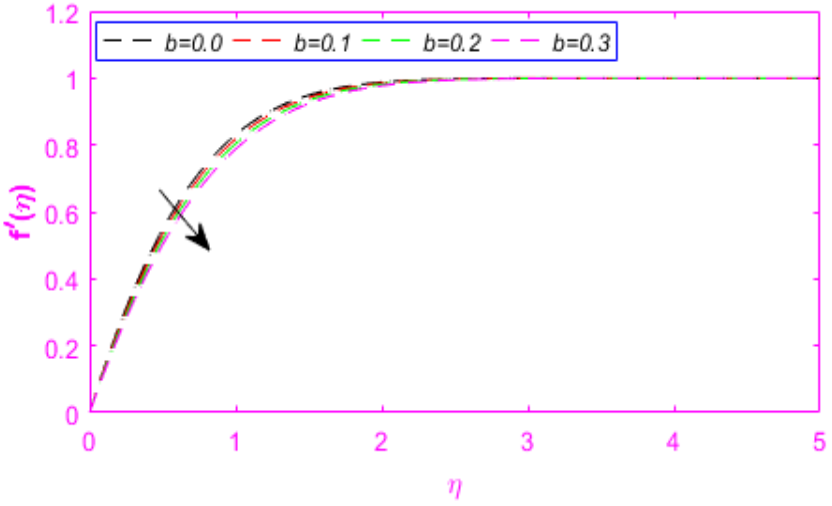

FIGURE 4.3: Variation of squeezed flow index.

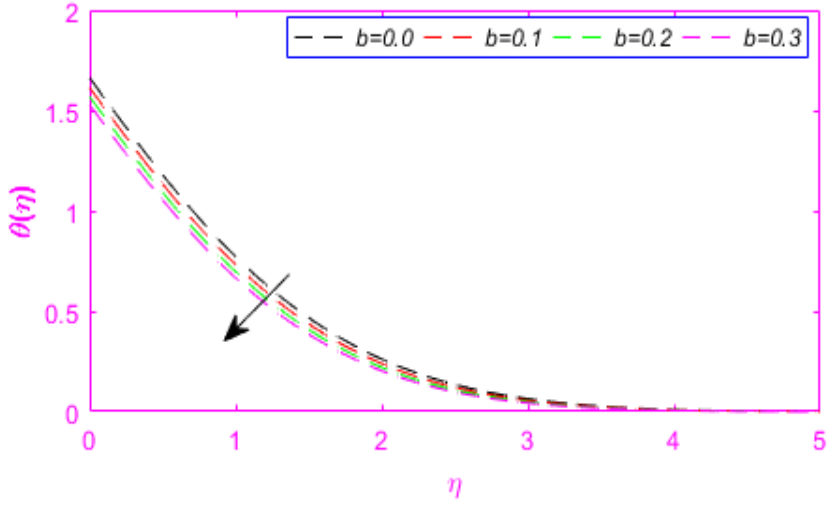

FIGURE 4.4: Variation of squeezed flow index.

4.5.4 Effect of Magnetic Parameter

Effect of the magnetic parameter M on the velocity profile will be analysed in the following discussion. In Figure 4.5, it is shown that if we increase the magnetic number, the velocity profile also increases. When the magnetic number gets larger values, the fluid is normally assumed to be slowed down. However, Figure 4.5 reflects an opposite behaviour. It is due to the squeezing phenomenon which has more stronger effect than the magnetic field. In case of temperature profile, when we increase the magnetic number, a decreasing trend can be noticed in Figure 4.6.

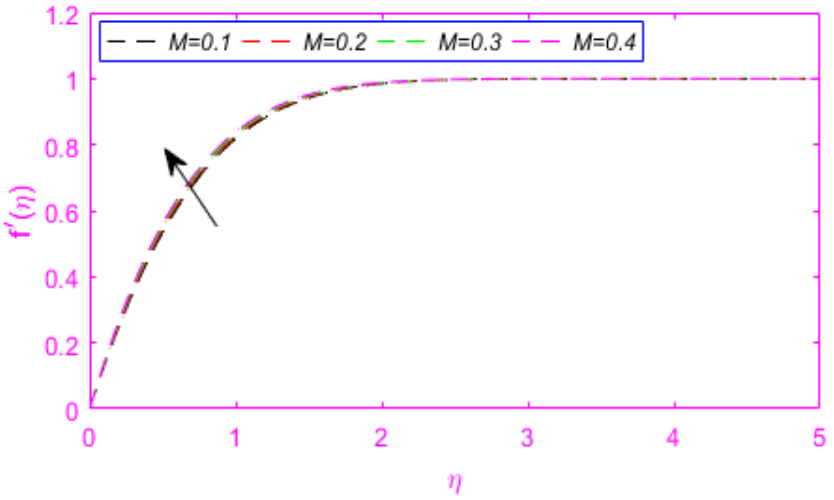

FIGURE 4.5: Variation of magnetic number.

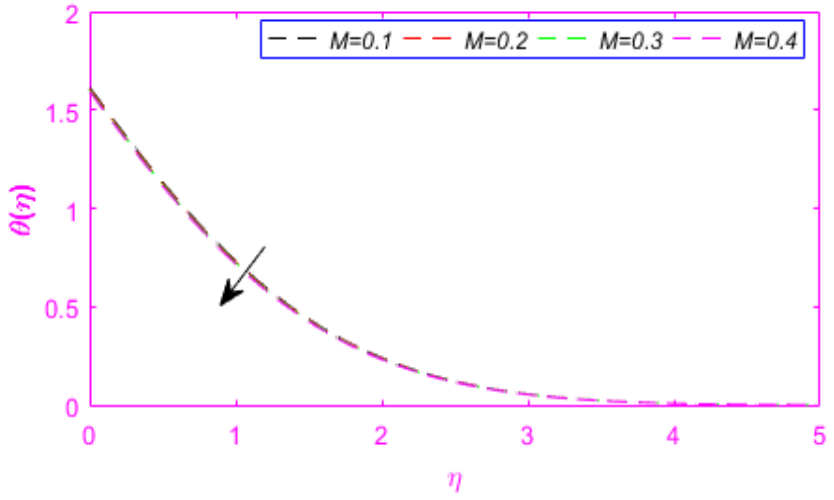

FIGURE 4.6: Variation of magnetic number.

4.5.5 Effect of Power Law Index

To show the impact of the power-law index n on the velocity and temperature profiles, Figures 4.7 and 4.8 have been included. A increasing the velocity behaviour and decreasing the temperature profile can be observed due to the effect of shear thinning its viscosity decreases with shear strain.

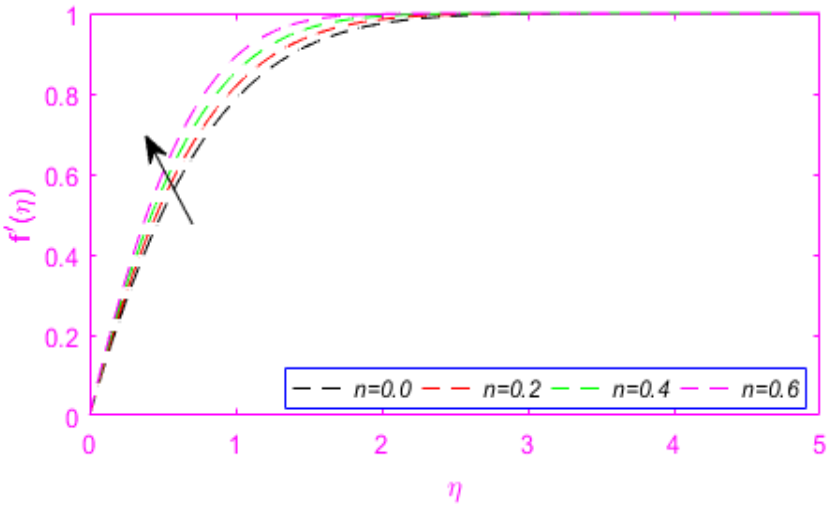

FIGURE 4.7: Variation of power-law index.

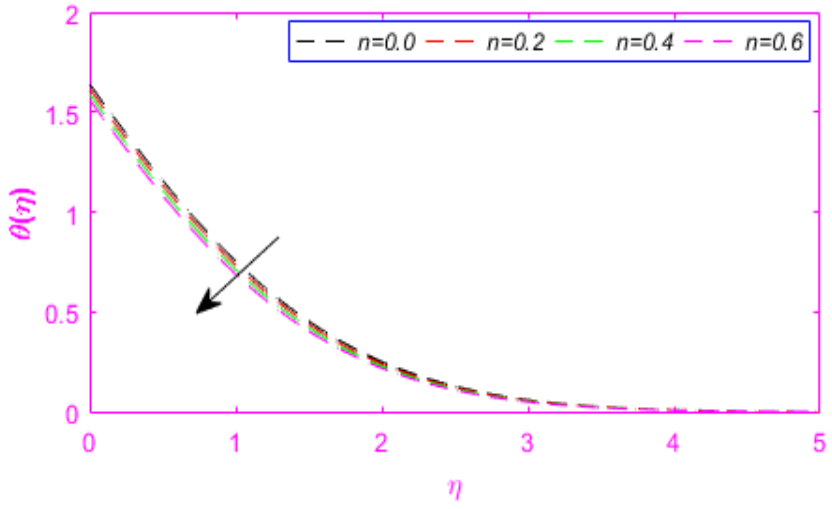

FIGURE 4.8: Variation of power-law index.

4.5.6 Effect of Permeable Velocity

Figures 4.9 and 4.10 show the effects of the permeable velocity f_0 on the velocity and temperature profiles. The velocity profile can be seen to reduce if the permeable velocity f_0 bears an increment for the suction case. This behaviour happens due to the fact that suction is responsible for pushing the fluid towards the sensor surface. The permeable velocity leaves a similar effect on the temperature distribution as presented in Figure 4.10.

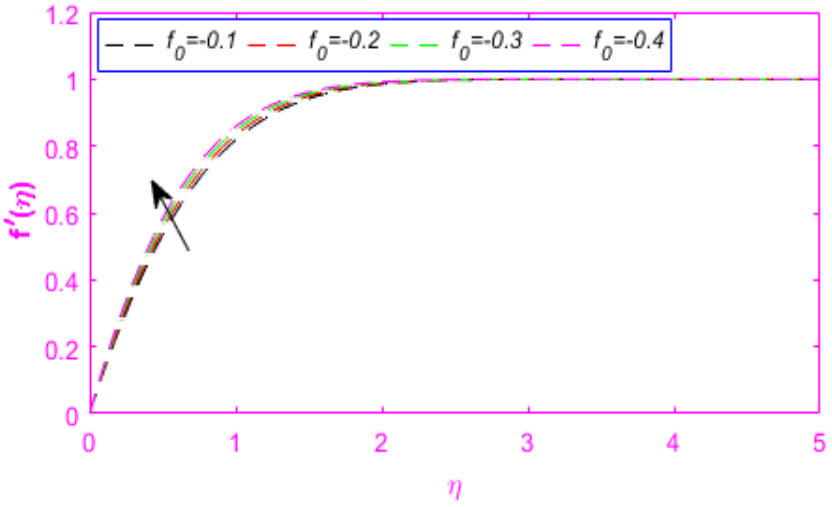

FIGURE 4.9: Variation of permeable velocity.

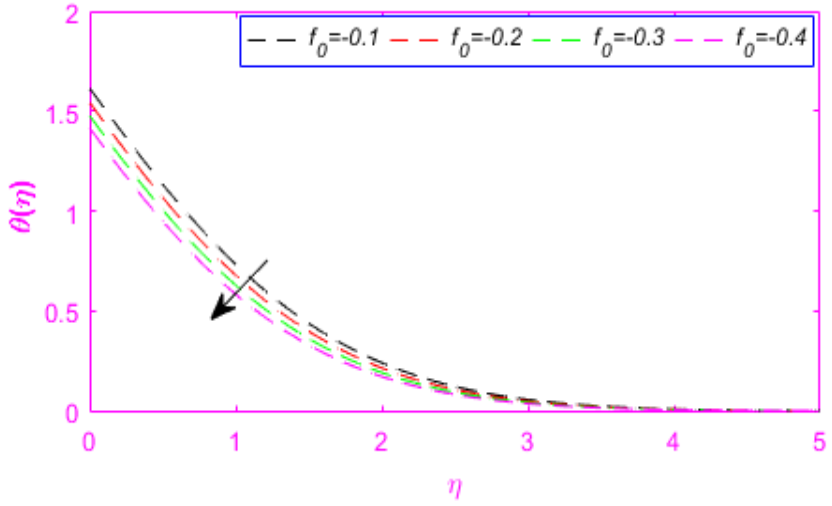

FIGURE 4.10: Variation of permeable velocity.

4.5.7 Effect of Prandtl Number and ϵ

Figure 4.11 shows the Prandtl number Pr effect on the temperature. Prandtl number as defined by the ratio of momentum diffusivity to the thermal diffusivity. The temperature profile is marked to decline for the increasing values of the prandtl number. Figure 4.12 shows an increasing behaviour of the temperature for rising function of ϵ. It happens because for higher values of ϵ, the kinetic energy gets larger which causes the temperature to rise.

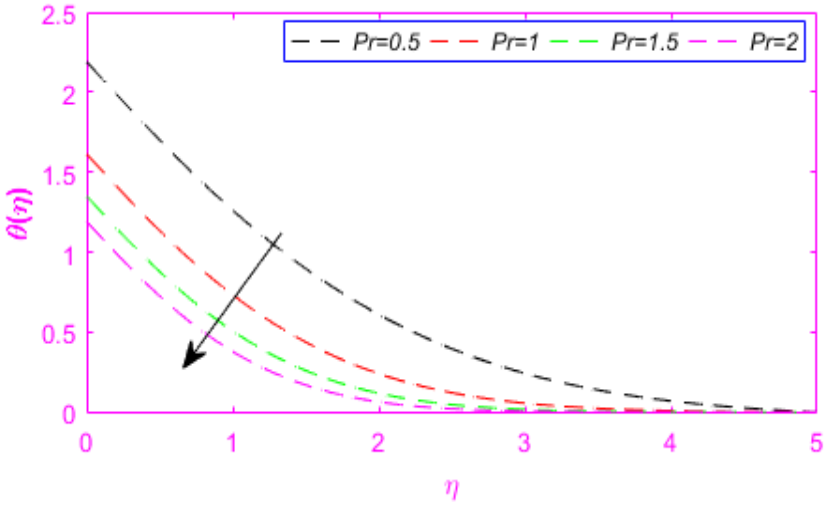

FIGURE 4.11: Variation of Prandtl number.

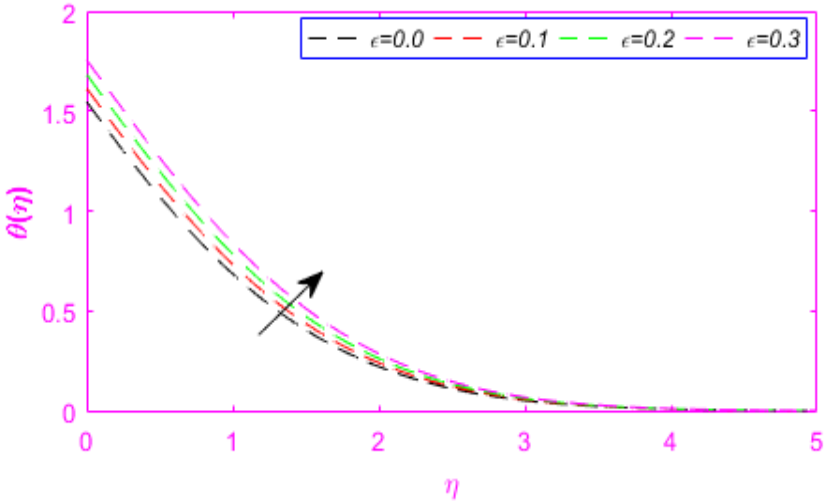

FIGURE 4.12: Variation of small parameter.

4.5.8 Effect of Thermal Radiation

Figure 4.13 shows the behaviour of thermal radiation on the temperature profile. The temperature profile can be observed to rise as an leading values of the thermal radiation. The thickness of boundary layer is also increased.

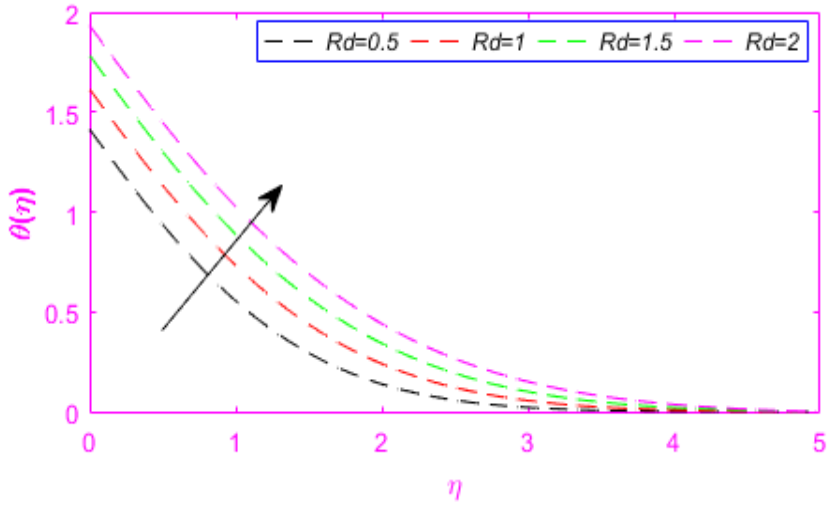

FIGURE 4.13: Variation of thermal radiation.

Chapter 5

Conclusion

In this very brief chapter, the thesis has been concluded with main focus on the crucial findings. The key findings have been listed below.

The thermal radiation is observed to decrease the Nusselt number, significantly, in all the cases. Keeping all the other parameters fixed, the radiation parameter is observed to decrease the Nusselt number. By keeping the radiation parameter fixed, the Nusselt number Nu_x is observed to decline by increasing the values of ϵ and the Weissenberg number W_e. By keeping the radiation parameter fixed, the Nusselt number is observed to rise by increasing the values of permeable velocity f_0, Prandtl number, squeezed flow index, magnetic number and power-law index. The thermal radiation parameter does not seem to affect the skin-friction coefficient in general. The thermal radiation parameter is found to cause a rise in the temperature.

Bibliography

[1] D. F. Moore, "A review of squeeze films," *Wear*, vol. 8, no. 4, pp. 245–263, 1965.

[2] C. Y. Wang, "The squeezing of a fluid between two plates," *Journal of Applied Mechanics*, vol. 43, no. 4, pp. 579–583, 1976.

[3] C. Y. Wang, "Arbitrary squeezing of fluid from a tube at low squeeze numbers," *Zeitschrift für angewandte Mathematik und Physik ZAMP*, vol. 31, no. 5, pp. 620–627, 1980.

[4] R. Usha, R. Sridharan, "Arbitrary squeezing of a viscous fluid between elliptic plates," *Fluid Dynamics Research*, vol. 18, no. 1, pp. 35–51, 1996.

[5] E. Magyari, B. Keller, "Heat and mass transfer in the boundary layers on an exponentially stretching continuous surface," *Journal of Physics D: Applied Physics*, vol. 32, no. 5, pp. 577–585, 1999.

[6] A. M. Rohni, S. Ahmad, and I. Pop, "Flow and heat transfer over an unsteady shrinking sheet with suction in nanofluids," *International Journal of Heat and Mass Transfer*, vol. 55, no. 7-8, pp. 1888–1895, 2012.

[7] S. Mahgoub, "Forced convection heat transfer over a flat plate in a porous medium," *Ain Shams Engineering Journal*, vol. 4, no. 4, pp. 605–613, 2013.

[8] M. Khan, M. Malik, T. Salahuddin, and I. Khan, "Heat transfer squeezed flow of Carreau fluid over a sensor surface with variable thermal conductivity: a numerical study," *Results in Physics*, vol. 6, pp. 940–945, 2016.

[9] M. Mahmood, S. Asghar, and M. Hossain, "Squeezed flow and heat transfer over a porous surface for viscous fluid," *Heat and Mass Transfer*, vol. 44, no. 2, pp. 165–173, 2007.

[10] J. R. Lin, R. F. Lu, and W. H. Liao, "Analysis of magneto-hydrodynamic squeeze film characteristics between curved annular plates," *Industrial Lubrication and Tribology*, vol. 56, no. 5, pp. 300–305, 2004.

[11] E. A. Hamza, "The magnetohydrodynamic effects on a fluid film squeezed between two rotating surfaces," *Journal of Physics D: Applied Physics*, vol. 24, no. 4, pp. 547–554, 1991.

[12] A. R. A. Khaled and K. Vafai, "Hydromagnetic squeezed flow and heat transfer over a sensor surface," *International Journal of Engineering Science*, vol. 42, no. 5-6, pp. 509–519, 2004.

[13] A. M. Siddiqui, S. Irum, and A. R. Ansari, "Unsteady squeezing flow of a viscous mhd fluid between parallel plates, a solution using the homotopy perturbation method," *Mathematical Modelling and Analysis*, vol. 13, no. 4, pp. 565–576, 2008.

[14] T. Hayat, A. Qayyum, and A. Alsaedi, "MHD unsteady squeezing flow over a porous stretching plate," *The European Physical Journal Plus*, vol. 128, no. 12, pp. 128–157, 2013.

[15] N. Ahmed, H. Kalita, and D. Barua, "Unsteady MHD free convective flow past a vertical porous plate immersed in a porous medium with Hall current, thermal diffusion and heat source," *International Journal of Engineering, Science and Technology*, vol. 2, no. 6, pp. 59–74, 2010.

[16] M. M. Sohn and C. W. Chen, "Microconvective thermal conductivity in disperse two-phase mixtures as observed in a low velocity couette flow experiment," *Journal of Heat Transfer*, vol. 103, no. 1, pp. 47–51, 1981.

[17] O. D. Makinde, "Free convection flow with thermal radiation and mass transfer past a moving vertical porous plate," *International Communications in Heat and Mass Transfer*, vol. 32, no. 10, pp. 1411–1419, 2005.

[18] T. Hayat, A. Qayyum, F. Alsaadi, M. Awais, and A. M. Dobaie, "Thermal radiation effects in squeezing flow of a jeffery fluid," *The European Physical Journal Plus*, vol. 128, no. 8, pp. 1–85, 2013.

[19] S. A. Hussain, S. Muhammad, G. Ali, S. I. A. Shah, M. Ishaq, Z. Shah, H. Khan, M. Tahir, and M. Naeem, "A bioconvection model for squeezing flow between parallel plates containing gyrotactic microorganisms with impact of thermal radiation and heat generation/absorption," *Journal of Advances in Mathematics and Computer Science*, pp. 1–22, 2018.

[20] M. Awais, T. Hayat, and A. Alsaedi, "Investigation of heat transfer in flow of burgers fluid during a melting process," *Journal of the Egyptian Mathematical Society*, vol. 23, no. 2, pp. 410–415, 2015.

[21] S. Muhammad, S. I. A. Shah, G. Ali, M. Ishaq, S. A. Hussain, and H. Ullah, "Squeezing nanofluid flow between two parallel plates under the influence of MHD and thermal radiation," *Asian Research Journal of Mathematics*, pp. 1–20, 2018.

[22] C. T. Nguyen, G. Roy, C. Gauthier, and N. Galanis, "Heat transfer enhancement using al2o3–water nanofluid for an electronic liquid cooling system," *Applied Thermal Engineering*, vol. 27, no. 8-9, pp. 1501–1506, 2007.

[23] C. Datt, G. J. Elfring, "Dynamics and rheology of particles in shear-thinning fluids," *Journal of Non-Newtonian Fluid Mechanics*, vol. 262, pp. 107–114, 2018.

[24] K. G. Kumar, B. J. Gireesha, M. R. Krishanamurthy, and N. G. Rudraswamy, "An unsteady squeezed flow of a tangent hyperbolic fluid over a sensor surface in the presence of variable thermal conductivity," *Results in Physics*, vol. 7, pp. 3031–3036, 2017.

[25] N. S. Akbar, S. Nadeem, R. U. Haq, and Z. Khan, "Numerical solutions of magnetohydrodynamic boundary layer flow of tangent hyperbolic fluid towards a stretching sheet," *Indian journal of Physics*, vol. 87, no. 11, pp. 1121–1124, 2013.

[26] T. Hayat, S. Qayyum, B. Ahmad, and M. Waqas, "Radiative flow of a tangent hyperbolic fluid with convective conditions and chemical reaction," *The European Physical Journal Plus*, vol. 131, no. 12, p. 422, 2016.

[27] M. Malik, T. Salahuddin, A. Hussain, and S. Bilal, "MHD flow of tangent hyperbolic fluid over a stretching cylinder: Using keller box method," *Journal of magnetism and magnetic materials*, vol. 395, pp. 271–276, 2015.

[28] N. S. Akbar, Z. H. Khan, "Effect of variable thermal conductivity and thermal radiation with CNTS suspended nanofluid over a stretching sheet with convective slip boundary conditions: Numerical study," *Journal of Molecular Liquids*, vol. 222, pp. 279–286, 2016.

[29] N. Saidulu, T. Gangaiah, and A. V. Lakshmi, "Inclined magnetic field and viscous dissipation effects on tangent hyperbolic nanofluid flow with zero normal flux of nanoparticles at the stretching surface," *European Journal of Advances in Engineering and Technology*, vol. 5, no. 3, pp. 142–150, 2018.

[30] W. Ibrahim, "Magnetohydrodynamics (MHD) flow of a tangent hyperbolic fluid with nanoparticles past a stretching sheet with second order slip and convective boundary condition," *Results in Physics*, vol. 7, pp. 3723–3731, 2017.

[31] M. Khan, A. Hussain, M. Malik, T. Salahuddin, and F. Khan, "Boundary layer flow of MHD tangent hyperbolic nanofluid over a stretching sheet: A numerical investigation," *Results in physics*, vol. 7, pp. 2837–2844, 2017.

[32] R. U. Haq, S. Nadeem, Z. Khan, and N. Noor, "MHD squeezed flow of water functionalized metallic nanoparticles over a sensor surface," *Physica E: Low-dimensional Systems and Nanostructures*, vol. 73, pp. 45–53, 2015.

[33] T. Salahuddin, M. Malik, A. Hussain, S. Bilal, M. Awais, and I. Khan, "MHD squeezed flow of Carreau-Yasuda fluid over a sensor surface," *Alexandria Engineering Journal*, vol. 56, no. 1, pp. 27–34, 2017.

[34] S. R. Rout, B. C. Mishra, "Thermal energy transport on MHD nanofluid flow over a stretching surface: A comparative study," *Engineering science and technology, an international journal*, vol. 21, no. 1, pp. 60–69, 2018.

[35] T. Hayat, M. Hussain, S. Nadeem, A. Alsaedi, and S. Obaidat, "Squeezed flow and heat transfer in a second grade fluid over a sensor surface," *Thermal Science*, vol. 18, no. 2, pp. 357–364, 2014.

[36] J. Homola, "Present and future of surface plasmon resonance biosensors," *Analytical and bioanalytical chemistry*, vol. 377, no. 3, pp. 528–539, 2003.

[37] M. Piliarik, H. Vaisocherová, and J. Homola, "A new surface plasmon resonance sensor for high-throughput screening applications," *Biosensors and Bioelectronics*, vol. 20, no. 10, pp. 2104–2110, 2005.

[38] J. L. Say, H. Sakslund, M. F. Tomasco, J. D. Audett, H. Cho, D. O. Yamasaki, and A. Heller, "Mass transport limited in VIVO analyte sensor," Nov. 25 2003.

[39] R. Kandasamy and R. Muhammad, "Thermal radiation energy on squeezed MHD flow of Cu, Al2O3 and CNTS-nanofluid over a sensor surface," *Alexandria Engineering Journal*, vol. 55, no. 3, pp. 2405–2421, 2016.

[40] M. Khan, M. Malik, T. Salahuddin, and I. Khan, "Heat transfer squeezed flow of Carreau fluid over a sensor surface with variable thermal conductivity: a numerical study," *Results in physics*, vol. 6, pp. 940–945, 2016.

[41] J. M. Cencel, Y. A Cimbala, "Fluid mechanics–fundamentals and applications," pp. 1–1031, 2006.

[42] R. K. Bansal, "A textbook of fluid mechanics and hydraulic machines," pp. 1–287, 2004.

[43] J. W. Sons, "Fundamentals of fluid mechanics," vol. 6, pp. 1–783, 1997.

[44] G. Z. Zakir Ullah, "Lie group analysis of magnetohydrodynamic tangent hyperbolic fluid flow towards a stretching sheet with slip conditions," *Heliyon*, vol. 3, pp. 2–11, 2017.

[45] E. Angelovska, "Difference between conduction and convection," vol. 3, pp. 1–4, 2018.

[46] D. Johan and J. R. Anderson, "Ludwig prandtl's boundary layer," vol. 58, no. 12, pp. 42–48, 2005.